THE JOURNAL OF BIOLOGICAL CHEMISTRY VOL. 291, NO. 20, pp. 10586–10601, May 13, 2016

The Gas6-Axl Protein Interaction Mediates Endothelial Uptake of Platelet Microparticles*

Received for publication, October 23, 2015, and in revised form, March 21, 2016 Published, JBC Papers in Press, March 22, 2016, DOI 10.1074/jbc.M115.699058

Kaisa E. Happonen[‡1], Sinh Tran[‡], Matthias Mörgelin[§], Raja Prince[¶‖], Sara Calzavarini[¶‖], Anne Angelillo-Scherrer[¶‖], and Björn Dahlbäck[‡]

From the [‡]Department of Translational Medicine, Division of Clinical Chemistry, Lund University, SE-20502 Malmö Sweden, the [§]Department of Clinical Sciences, Division of Infection Medicine, Lund University, SE-22185 Lund, Sweden, the [¶]University Clinic of Hematology and Central Hematology Laboratory, Bern University Hospital, Bern CH-3010, Switzerland, and the [‖]Department of Clinical Research, University of Bern, Bern CH-3010, Switzerland

Upon activation, platelets release plasma membrane-derived microparticles (PMPs) exposing phosphatidylserine on their surface. The functions and clearance mechanism of these microparticles are incompletely understood. As they are pro-coagulant and potentially pro-inflammatory, rapid clearance from the circulation is essential for prevention of thrombotic diseases. The tyrosine kinase receptors Tyro3, Axl, and Mer (TAMs) and their ligands protein S and Gas6 are involved in the uptake of phosphatidylserine-exposing apoptotic cells in macrophages and dendritic cells. Both TAMs and their ligands are expressed in the vasculature, the functional significance of which is poorly understood. In this study, we investigated how vascular TAMs and their ligands may mediate endothelial uptake of PMPs. PMPs, generated from purified human platelets, were isolated by ultracentrifugation and labeled with biotin or PKH67. The uptake of labeled microparticles in the presence of protein S and Gas6 in human aortic endothelial cells and human umbilical vein endothelial cells was monitored by flow cytometry, Western blotting, and confocal/electron microscopy. We found that both endothelial cell types can phagocytose PMPs, and by using TAM-blocking antibodies or siRNA knockdown of individual TAMs, we show that the uptake is mediated by endothelial Axl and Gas6. As circulating PMP levels were not altered in *Gas6*$^{-/-}$ mice compared with *Gas6*$^{+/+}$ mice, we hypothesize that the Gas6-mediated uptake is not a means to clear the bulk of circulating PMPs but may serve to locally phagocytose PMPs generated at sites of platelet activation and as a way to effect endothelial responses.

Platelets are key players in the regulation of hemostasis, coagulation, and thrombosis. Upon activation, platelets shed small, 100-nm to 1-μm vesicles, often referred to as microparticles (PMPs),[2] microvesicles or extracellular vesicles. These PMPs expose a hundredfold more phosphatidylserine (PS) on their surface than activated platelets themselves, and by supporting the activation of factor X and prothrombin, they are highly pro-coagulant (1). However, the activated protein C system together with protein S has the ability to down-regulate their pro-coagulant phenotype, thereby creating a balance between coagulation and anti-coagulation (2). In addition to plasma membrane-derived PMPs, platelets also shed exosomes upon activation. These vesicles are usually derived from multivesicular bodies within the cell and carry different cargo and surface composition than PMPs. Furthermore, platelet exosomes are generally smaller than PMPs (3). However, using currently available methods, PMPs and platelet-derived exosomes are still difficult to analytically distinguish from one another. Furthermore, whether the pool of CD41-positive PMPs in the circulation is derived from platelets upon activation or directly from megakaryocytes is still unclear (4, 5).

Flow cytometric studies have shown that PMPs contribute to more than 70% of the circulating microparticle (MP) pool (6, 7), but the number has recently been challenged by an electron microscopy study that suggested ~25% of the MPs to be PMPs (8). However, their abundance may be further increased during several disease states (9, 10). PMPs have disease-causing abilities apart from triggering thrombosis, *e.g.* as demonstrated by Boilard *et al.* (11), who showed that PMPs trigger inflammatory responses in synovial fibroblasts and contribute to the pathogenesis of inflammatory arthritis. In addition, PMPs induce a pro-inflammatory response in endothelium, by up-regulating adhesion molecule expression and cytokine secretion (12, 13), effects attributed to PMP-derived arachidonic acid (12) and the chemokine RANTES (regulated on activation, normal T-cell expressed and secreted) (14). In contrast, PMPs induce immunosuppressive effects in macrophages and dendritic cells (15) and induce the differentiation of $CD4^+$ into $Foxp^3$ regulatory T-cells (16), which suggests they may also down-regulate inflammation.

Labeled PMPs injected into rabbits were found to be cleared in less than 10 min (17), whereas the half-life of transfused

* This work was supported by grants from Swedish Research Council (to B. D.), the Heart-Lung Foundation (to B. D.), the Söderberg's Foundation (to B. D.), Skåne University Hospital Research Funds (to B. D.) and grants from the Foundations of Greta and Johan Kock (to K. E. H.), Alfred Österlund (to K. E. H.), Tore Nilsson (to K. E. H.), Prof. Nanna Svartz (to K. E. H.), Apotekare Hedberg (to K. E. H.), and the Royal Physiographic Society in Lund (to K. E. H.). The authors declare that they have no conflicts of interest with the contents of this article.

[1] To whom correspondence should be addressed: Lund University, Department of Translational Medicine, Clinical Chemistry, Wallenberg laboratory, Inga Marie Nilssons gata 53, SE-20502 Malmö, Sweden. E-mail: kaisa.happonen@med.lu.se.

[2] The abbreviations used are: PMP, platelet microparticle; PS, phosphatidylserine; MP, microparticle; HAEC, human aortic endothelial cell; HUVEC, human umbilical vein endothelial cell; TAM, Tyro3, Axl, and Mer; eryMP, erythrocyte-derived microparticle; PE, phosphatidylethanolamine; PC, phosphatidylcholine; s, soluble.

PMPs in humans was estimated to be 5.8 h (4). Macrophages have been shown to ingest PMPs in a lactadherin-dependent manner, and splenectomized mice showed an increase in the amount of circulating PMPs, indicating that the spleen is an important site of clearance (18). Furthermore, β-2-glycoprotein was shown to serve as an inducer of PMP phagocytosis by THP-1-derived macrophages (19). In addition, human umbilical vein endothelial cells (HUVECs) and brain endothelial cells have been shown to phagocytose PMPs, the former in a Del-1-dependent manner (20–22). Activated neutrophils can also ingest PMPs, an uptake triggered by 12(*S*)-hydroxyeicosatetranoic acid (23). This shows that there are several overlapping mechanisms of PMP removal from the circulation, which may promote different cellular outcomes in the recipient cells.

Phagocytosis of PS-exposing apoptotic cells is mediated by several receptor-ligand systems, one of which is the TAM receptor-Gas6/protein S system. The members of the TAM receptor family, comprising Tyro3, Axl, and Mer, are predominantly known for their ability to induce phagocytosis of apoptotic cells in macrophages and dendritic cells (24, 25) as well as in Sertoli cells in the testis (26, 27), retinal pigment epithelial cells (28), and microglia (29). Importantly, this inhibits inflammatory responses by modulating the activation of NF-κB and inducing the expression of silencers of cytokine secretion 1 and 3 (30, 31). The TAMs are activated by two main ligands, Gas6 and protein S, each containing a γ-carboxylated GLA domain, which allows them to bind negatively charged phospholipids, such as PS, exposed among others on apoptotic cells and PMPs. This interaction thus promotes an interaction between the TAM-expressing cell and the PS-exposing surface (32).

Both Axl and Mer are expressed in endothelium, where they modulate angiogenesis (33–35) and induce cell survival (36, 37). Moreover, endothelial Axl activation by Gas6 increases tissue factor expression, thus promoting thrombogenesis (38, 39). Gas6 deficiency has been shown to protect mice against thrombosis, an effect that, in addition to endothelial modulation, may be due to a direct platelet-stimulatory effect of Gas6 (40). Further roles for endothelial TAM receptors remain to be described.

In this study, we have investigated the involvement of endothelial TAM receptors in the uptake on PS-exposing PMPs and the selectivity of the TAM ligands for this uptake. We show that two different primary endothelial cell types efficiently phagocytose PMPs in an Axl-Gas6-dependent manner. This provides a novel role for endothelial TAM receptors and strengthens the role of Axl as a phagocytic receptor.

Materials and Methods

Cell Culture—Human umbilical vein endothelial cells (HUVEC, Life Technologies, Inc.) and human aortic endothelial cells (HAEC, Life Technologies, Inc.) were cultured on gelatin-coated flasks/plates in M200 medium supplemented with low serum growth supplement (Life Technologies, Inc.) as well as 50 units/ml penicillin and 50 μg/ml streptomycin. THP-1 cells were cultured in RPMI 1640 medium supplemented with 10% fetal calf serum (FCS), 2 mM L-glutamine, 50 units/ml penicillin, and 50 μg/ml streptomycin. All cells were cultured in a humidified chamber with 5% CO_2 at 37 °C.

Proteins—Rabbit anti-protein S (A0384, Dako) and rabbit anti-Gas6 (0005, homemade) were labeled with Alexa Fluor 488 using the microscale protein labeling kit (A30006) from Life Technologies, Inc. Soluble Axl (sAxl) comprising the extracellular domain alone was expressed and purified as described elsewhere (41). Human α-thrombin was prepared from prothrombin as described previously (42). A commercially available Gas6, which was shown to lack proper γ-carboxylation, was from R&D Systems (46).

Purification of Gas6—Recombinant human Gas6 was expressed in HEK293 cells in the presence of 10 μg/ml vitamin K and purified as described previously (43) with the following modifications. Expression media with recombinant human Gas6 were supplemented with 1 mM PMSF and 50 μg/ml soybean trypsin inhibitor, centrifuged at 2500 rpm for 10 min at 4 °C, and filtered through a 0.45-μm membrane. A DEAE-Sephacel matrix (150 ml, GE Healthcare) equilibrated with 20 mM Tris-HCl, pH 8.0, 50 mM NaCl was added and incubated with the cell medium for 2 h at 4 °C with stirring. The unbound fraction was collected and diluted 1:2 with filtered distilled water. A fresh DEAE-Sephacel resin equilibrated in 20 mM Tris-HCl, pH 8.0, 20 mM NaCl was added, and incubation was continued for 2 h at 4 °C. The resin was packed into a column and washed with 20 mM Tris-HCl, pH 8.0, 20 mM NaCl. Bound proteins were eluted with a 20–500 mM NaCl gradient in 20 mM Tris-HCl, pH 8.0. Gas6-containing fractions were collected, pooled, and concentrated on 10-kDa molecular mass cutoff spin columns (Amicon). The concentrated sample was separated on a Superdex 200 column (GE Healthcare) and eluted with 100 mM NaCl in 20 mM Tris-HCl, pH 8.0. Gas6-containing fractions were pooled and stored in aliquots at −70 °C after verification of protein purity.

Purification of Protein S—Protein S was purified from fresh-frozen human plasma according to a previously published method (44) with the following changes. The $BaCl_2$ precipitate was dissolved in 0.2 M EDTA containing 10 mM benzamidine and 0.1 mM PMSF, after which ammonium sulfate was added stepwise to 40% saturation. The mixture was stirred overnight at 4 °C and then centrifuged at 2400 × *g* for 20 min at 4 °C to remove precipitated proteins. Ammonium sulfate was added to the supernatant to a final concentration of 67%, and the sample was stirred at 4 °C for 1 h to induce precipitation of vitamin K-dependent proteins. The precipitate was collected by centrifugation at 15,000 × *g* for 20 min at 4 °C, after which it was dissolved in 0.1 M sodium phosphate, pH 6.0, 10 mM benzamidine, 0.1 mM PMSF, 1% Tween 20. The sample was dialyzed overnight against 0.1 M sodium phosphate, pH 6.0, 10 mM benzamidine, 0.1 mM PMSF with three buffer changes. After filtering through a 0.45-μm filter, the sample was applied to a DEAE-Sephacel matrix (GE Healthcare) equilibrated with 0.1 M sodium phosphate, pH 6.0, 10 mM benzamidine, 0.1 mM PMSF. The column was washed with 0.1 M sodium phosphate, pH 6.0, 10 mM benzamidine, 0.1 mM PMSF, 1% Tween 20, and 0.1 M sodium phosphate, pH 6.0, 100 mM NaCl, 10 mM benzamidine, 0.1 mM PMSF. Bound proteins were then eluted with a linear gradient of 100–700 mM NaCl in 0.1 M sodium phosphate, pH 6.0, 10 mM benzamidine, 0.1 mM PMSF after which free protein S-containing fractions were pooled. The sample was dialyzed

against 20 mM Tris-HCl, pH 7.5, 100 mM NaCl, 10 mM benzamidine, 0.1 mM PMSF and passed through a Blue-Sepharose column (GE Healthcare) equilibrated with 20 mM Tris-HCl, pH 7.5, 1 mM EDTA, 100 mM NaCl, 10 mM benzamidine, 0.1 mM PMSF. The unbound fraction containing protein S was collected and passed through a 5-ml HiTrap column (GE Healthcare) coupled with an in-house monoclonal antibody against C4b-binding protein (C4BP, MK104) to ensure complete removal of C4BP-bound protein S. The flow-through was further purified on a HiTrap column coupled with an in-house monoclonal antibody against protein S (MK21) (45). The pure protein S was dialyzed against TBS containing 2 mM $CaCl_2$ and stored in aliquots at −80 °C.

Purification of sMer—cDNA comprising amino acids 1–490 of the Mer extracellular domain was cloned into a pcDNA3.1 vector with a thrombin cleavage site and a His_6 sequence at the 3′ end (41). The vector was transfected into HEK293 cells, and stably expressing clones were selected using hygromycin selection medium. Conditioned medium was passed through a Ni^{2+}-chelated HisTrap Excel column (GE Healthcare) using an Äkta Avant system. The column wash washed with TBS (50 mM Tris-HCl, pH 8.0, 150 mM NaCl) followed by 50 mM Tris-HCl, pH 8.0, 1000 mM NaCl, and bound proteins were eluted using an imidazole gradient. sMer-containing fractions were pooled and dialyzed against TBS after which the His_6 epitope was removed by adding thrombin to 3 μg/ml and incubating the sample for 2 h at 37 °C. The sample was passed through the HisTrap excel column again, and the flow-through was collected. Thrombin was removed by passing the sample through a benzamidine column (GE Healthcare). The sMer-containing pool was aliquoted and stored at −80 °C.

Platelet Microparticle Preparation and Labeling—Platelets were purified from pooled fresh human citrated blood collected from healthy volunteers as described (2) with the permission of the local ethical board at Lund University. MP formation was induced by stimulating platelets at a concentration of 100×10^6/ml with 5.9 μM calcium ionophore (A23187, Life Technologies, Inc.) or 0.5 units/ml thrombin and 25 μg/ml collagen (Chrono-Log Corp.) in activation buffer (140 mM NaCl, 2.5 mM KCl, 0.1 mM $MgCl_2$, 3 mM $CaCl_2$, 60 mM Hepes, 0.5 mM NaH_2PO_4, 5.5 mM glucose, and 10 mM HCO_3, pH 7.4), for 25 min at 37 °C. Intact platelets were removed by centrifugation at 1500 × *g* for 10 min at 4 °C, and PMPs were collected by centrifuging the supernatant at 100,000 × *g* for 30 min at 4 °C. The pelleted PMPs were either resuspended in 5 mg/ml BSA in PBS and frozen in aliquots at −80 °C or fluorescently labeled using the PKH67 green fluorescent labeling kit (Sigma). Alternatively, PMPs were biotinylated by adding EZ-link Sulfo-NHS-LC-Biotin (Thermo Scientific) during the ionophore stimulation. Excess non-reacted reagent was adsorbed by adding glycine to 100 mM, after which intact platelets were removed as above and the PMPs were centrifuged at 100,000 × *g* for 30 min at 4 °C. PMPs were labeled with anti-CD41a PerCP-Cy5.5 (340931, BD Biosciences) for counting by flow cytometry using an FC500 flow cytometer (Beckman Coulter). Count Bright absolute counting beads (C36950, Life Technologies, Inc.) were used as reference. Flow cytometry data analysis was carried out using the FlowJo 8.8.7 software (Tree Star Inc). PS exposure was verified by staining the PMPs with FITC-conjugated lactadherin (Hematologic Technologies Inc.), and biotinylation efficiency was evaluated by staining the PMPs with streptavidin-Alexa Fluor 488 (Life Technologies, Inc.). Alternatively, unlabeled and biotinylated PMPs were lysed in RIPA buffer (50 mM Tris-HCl, pH 8.0, 150 mM NaCl, 0.1% SDS, 1% Triton X-100, 0.5% deoxycholate supplemented with HALT protease and phosphatase inhibitor mixture (Life Technologies, Inc.)) and analyzed with SDS-PAGE followed by Western blotting under reducing conditions. Blots were then probed for biotin using the Vectastain ABC kit (Vector Laboratories) to identify biotinylated proteins. Western blots were developed using an Immobilon Western Chemiluminescent HRP substrate (Millipore), imaged in the ChemiDoc MP system (Bio-Rad), and analyzed using ImageLab software (Bio-Rad). The size distribution of PMPs was evaluated using nanotracking analysis (NanoSight).

Preparation of Erythrocyte and THP1-derived MPs—Erythrocytes were purified from citrated blood by centrifugation at 250 × *g* for 15 min at room temperature. The plasma layer and buffy coat were removed, and erythrocytes were pooled. The erythrocytes were washed three times in activation buffer and pelleted at 2500 × *g* for 10 min. Erythrocyte MP (eryMP) formation was induced using the calcium ionophore A23187, and subsequent PKH67 labeling was carried out as described for the PMPs; alternatively, the particles were left unlabeled.

THP-1 cells were seeded at a concentration of 1×10^6 cells/ml in fresh-filtered (0.2 μm) RPMI 1640 medium supplemented with 10% FCS and 20 μg/ml LPS (O111:B4, Sigma) and incubated at 37 °C for 24 h. Intact cells were removed by centrifugation at 500 × *g* for 10 min followed by two centrifugations at 1500 × *g* for 10 min at room temperature. The supernatant was then ultracentrifuged at 100,000 × *g* to collect THP-1 MPs and labeled with PKH67 as for the PMPs.

Measuring PMPs in Mouse Plasma—*Gas6*$^{+/+}$ and *Gas6*$^{-/-}$ mice were progeny of the original colony (40), with a genetic mixed background of 50% 129/Sv × 50% C57Bl6/J. *Gas6*$^{-/-}$ ($n = 13$, 10 female, 3 male, mean age 13 weeks) and *Gas6*$^{+/+}$ ($n = 10$, 6 male, 4 female, mean age 10 weeks) mice were anesthetized by intraperitoneal injection of sodium pentobarbital (50 mg/ml, 150 mg/kg), after which blood was collected in acid citrate dextrose from the inferior vena cava. The blood was centrifuged at 750 rpm for 10 min (Thermo ALC PK13R centrifuge with rotor T516), and the platelet-rich plasma was collected. Platelets were removed by centrifugation at 2500 × *g* for 10 min at room temperature, and platelet removal was verified by flow cytometry. The remaining platelet-poor plasma was stained with bovine lactadherin-FITC (Hematologic Technologies Inc.) and rat anti-mouse CD41-PE (BD Biosciences). Samples were analyzed on a Beckman Coulter Gallios flow cytometer calibrated with Megamix-Plus FSC beads (BioCytex) and a Nano Size Standard (Spherotech) to monitor events in the range of 0.1–0.8 μm. This was shown to exclude events of intact platelets. Particles in this size range positive for CD41 were considered to be PMPs. To exclude that the signal was disturbed by aggregates of antibodies or lactadherin, platelet-poor plasma was treated with 0.2% Triton X-100 during staining, which completely removed all PMP signals observed in the

flow cytometer. Quantification of PMPs in the samples was performed by adding a known amount of calibration beads (Spherotech) to each sample. The Swiss Federal Veterinary Office approved the experiments.

Phospholipid Vesicle Preparation—Phospholipids (phosphatidylserine (PS), phosphatidylethanolamine (PE), and phosphatidylcholine (PC), all from Avanti Polar Lipids) were dissolved in 10:90 (v/v) methanol/chloroform solution. Mixtures of the lipids (20/20/60% PS/PE/PC or 20/80% PE/PC) (weight-based) were prepared in 10/90 methanol/chloroform and stored at −20 °C. Aliquots from the stocks were dried under N_2 and then resuspended in Tris-buffered saline (50 mM Tris-HCl, 150 mM NaCl, pH 8.0, TBS) at room temperature. Phospholipid vesicles were prepared by subjecting phospholipid mixtures to freeze-thaw cycles combined with extrusion using the Liposo-Fast basic extruder (Armatis, Germany) as described previously (47) using a membrane with a pore size of 100 nm. The phospholipid vesicles were used within 2 days.

TAM Expression Analysis Using Flow Cytometry—HAECs and HUVECs were grown to 90% confluency in 12-well cell culture plates. Cells were washed with PBS, detached using TrypLE Express, and washed once in full medium followed by one wash in 1% BSA in TBS. Anti-TAM antibodies (Axl, AF154 R&D Systems; Mer, ab52968 Abcam; Tyro3, AF859 R&D Systems) diluted 1:200 were preincubated with or without 10 μg/ml sTAMs in 50 μl of 1% BSA in TBS for 20 min. Cells were resuspended in the antibody mixtures and incubated on ice for 1 h. After two washes with 1% BSA in TBS, donkey anti-goat DyLight488 (Abcam) or goat anti-rabbit Alexa Fluor 488 (Invitrogen) was added, and incubation was continued for 1 h on ice in the dark. Cells were washed twice with 1% BSA in TBS, resuspended in 1% BSA in TBS, and analyzed immediately by flow cytometry (CyFlow Space, Partec). For monitoring TAM expression on platelets, TAM antibodies (as above) were incubated with 50,000 washed platelets in 1% BSA in PBS for 20 min at room temperature. Donkey anti-goat DyLight488 (Abcam) or goat anti-rabbit Alexa Fluor 488 (Invitrogen) was added together with 3 μl of anti-CD41a PerCP-Cy5.5, and incubation was continued for 20 min in the dark at room temperature. The samples were then diluted to 500 μl in 1% BSA in TBS and analyzed immediately on an FC500 flow cytometer (Beckman Coulter). The particles were gated for based on CD41a positivity.

Cell Surface Biotinylation for TAM Analysis—HAECs and HUVECs were grown to ~90% confluency in full medium. The plates were placed on ice and rinsed three times with ice-cold PBS. Sulfo-NHS-LC biotin was diluted to a concentration of 1 mM in PBS and incubated with the cells for 15 min on ice. Cells were washed three times with 100 mM glycine in PBS and lysed in RIPA buffer, after which cell residues were removed by centrifugation at 10,000 × *g* for 1 min at 4 °C. Axl and Mer were immunoprecipitated from protein G-Sepharose pre-cleared lysates corresponding to 100 μg of total protein with anti-Axl AF154 and anti-Mer MAB8912 (both from R&D Systems). Immunoprecipitated proteins were subjected to SDS-PAGE and Western blotting, and the membranes were probed for biotinylated proteins using the Vectastain ABC kit as above. The efficiency of the immunoprecipitation was evaluated by comparing Axl and Mer in lysates before and after immunoprecipitation, confirming that more than 97% of total Axl and Mer was indeed extracted.

Binding of Protein S and Gas6 to PMPs—PMPs (50,000/sample) were incubated with increasing amounts of protein S, Gas6, or a combination of both in 1% BSA in TBS supplemented with 2 mM $CaCl_2$ in a final volume of 50 μl. In some cases, samples were supplemented with annexin V (555416, BD Biosciences). To study the effect of calcium on the interaction, EDTA was added to 5 mM instead of $CaCl_2$. After 20 min of incubation at room temperature, Alexa Fluor 488-conjugated rabbit anti-protein S or rabbit anti-Gas6 was added to a concentration of 0.6 μg/ml together with 3 μl anti-CD41a-PerCPcy5.5, and incubation was continued for 20 min at room temperature in the dark. Samples were diluted to 500 μl in staining buffer and analyzed immediately on an FC500 flow cytometer. PMPs were gated on based on CD41a staining.

To evaluate the phospholipid dependence of the PMP-Gas6 interaction, PMPs were treated with 20 nM phospholipase A_2 in TBS + 2 mM $CaCl_2$ for 15 min at 37 °C. Gas6 at increasing concentrations was then added, and binding was monitored as above.

MP Uptake Using Western Blot—HUVECs were starved for 1 h in serum-free medium in a 12-well cell culture plate. Biotinylated PMPs (400,000/sample) were pre-incubated with increasing concentrations of Gas6 in serum-free medium for 20 min at room temperature after which they were added to the cells. After 1 h of incubation at 37 °C, the cells were washed with PBS and incubated with trypsin/EDTA for 5 min at 37 °C. Cells were detached by pipetting, transferred to tubes, and washed twice with PBS, followed by lysis in RIPA buffer containing HALT protease and phosphatase inhibitor mixture and 2 mM sodium orthovanadate. Protein concentrations were measured using the Pierce BCA assay (23227). Per sample, 10 μg of cell lysate was subjected to SDS-PAGE and Western blot under reducing conditions, followed by probing the membranes for biotinylated proteins using the Vectastain ABC kit as described above. β-Actin was detected as a loading control. Band intensities were quantified in the ImageLab software (Bio-Rad), and signals of biotin were normalized to the β-actin loading control.

MP Uptake Using Flow Cytometry—Gas6 at increasing concentrations was incubated with 800,000 PKH67-conjugated PMPs/THP-1 MPs or 100,000 eryMPs in 500 μl of serum-free medium for 20 min at room temperature after which the mixtures were added to cells pre-starved (1 h) in serum-free medium. After 1 h of incubation at 37 °C, cells were washed with PBS, incubated with trypsin/EDTA for 5 min at 37 °C, followed by two additional washes with PBS. Cells were resuspended in PBS and analyzed immediately using flow cytometry (CyFlow® Space, Partec). In experiments involving TAM knockdown using siRNA, cells were transfected with siRNA 48 h prior to uptake experiments, and proper knockdown was verified by Western blot in non-trypsinized cells transfected in parallel. To analyze the inhibitory effect of TAM-blocking antibodies, cells were pre-starved for 30 min in serum-free medium after which anti-TAMs were added to a final concentration of 5 μg/ml, and starvation was continued for an additional 30 min. PMPs were pre-incubated with a mixture of 0.25 μg/ml Gas6

and 5 μg/ml anti-TAMs prior to incubation with cells as above. To study the calcium dependence of the uptake, EDTA was added to the Gas6/MP mixtures to a concentration of 2.5 mM. When evaluating the requirement of Axl kinase activity, HAECs were pre-treated for 15 min with 0.5 μM R428 in starvation medium before adding PMP/Gas6 mixtures, which also were supplemented with R428. To analyze the dependence of actin and microtubule network remodeling for the uptake, HAECs were pre-starved for 1 h in serum-free medium in the presence of 0.3 μg/ml cytochalasin D (C2618, Sigma) or 0.3 μg/ml nocodazole (M1404, Sigma) prior to incubation with MP/Gas6 mixtures also containing either reagent.

MP Uptake Using Electron Microscopy—To study PMP internalization with electron microscopy, HAECs were grown to 90% confluency in 6-well plates. The cells were washed with PBS and starved in serum-free medium for 1 h. Biotinylated PMPs (800,000) were pre-incubated with 250 ng/ml Gas6 in starvation medium for 20 min after which they were incubated with the cells for 2 or 6 h at 37 °C. Cells were rinsed twice with PBS and fixed using 2.5% glutaraldehyde in 0.15 M sodium cacodylate buffer, pH 7.9. Specimens were then embedded in Epon 812 and ultrasectioned. For immunostaining, the sections were incubated with gold-conjugated streptavidin. Specimens were then examined at the Core Facility for Integrated Microscopy, Panum Institute, Copenhagen University, in a Philips/FEI CM100 BioTWIN transmission electron microscope. Images were recorded with a side-mounted Olympus Veleta camera.

Confocal Microscopy—HAECs were grown on gelatin-coated coverslips in 12-well cell culture plates and starved for 1 h in serum-free medium. Fluorescent PMPs (800,000) were incubated with 250 ng/ml Gas6 for 20 min at room temperature and added to the cells. After 4 h at 37 °C, the cells were washed, fixed in 4% paraformaldehyde in PBS for 20 min, washed with PBS, and blocked 15 min in 1% BSA in PBS. The coverslips were incubated with an anti-CD31 antibody (ab119339, Abcam) diluted in 1% BSA in PBS for 1 h at room temperature and following three washing steps, with a goat anti-mouse Alexa Fluor633 antibody (Life Technologies, Inc.) for 1 h at room temperature in the dark. The coverslips were washed with PBS and water and mounted onto Superfrost Plus microscopy slides using the ProLong Diamond Antifade Mountant with DAPI (Life Technologies, Inc.). The samples were visualized in an LSM 510 Meta confocal microscope (Zeiss) using a ×63 objective.

Cells treated with cytochalasin D or nocodazole were stained for actin and β-tubulin in Triton X-100 permeabilized cells using phalloidin Alexa Fluor 546 (A22283, Invitrogen) and mouse anti-β-tubulin (T5293, Sigma) followed by goat anti-mouse Alexa Fluor 488 (A11001, Invitrogen). The staining and visualization were performed as above.

Phosphorylation in HAEC by PMPs—HAECs were grown to 90% confluence in 6-well plates. Cells were rinsed with PBS and starved for 2 h in serum-free medium prior to stimulation. Gas6 (0, 100, or 200 ng/ml) was pre-incubated with 2×10^6 PMPs in 500 μl of serum-free medium for 20 min at room temperature, after which the mixes were added to the cells. Two wells were stimulated in parallel for each sample setup. After 15 min of incubation at 37 °C, the cells were placed on ice, rinsed with ice-cold PBS, and lysed in 200 μl of RIPA buffer (with HALT-protease and phosphatase inhibitor mixture as well as 2 mM sodium orthovanadate). Debris was removed by centrifugation at 10,000 × *g* for 5 min at 4 °C. Cell lysate corresponding to 150 μg of total protein was adjusted to 500 μl in lysis buffer and pre-cleared for 30 min with 30 μl of protein G-Sepharose suspension (Invitrogen). The supernatant was collected, and Axl was immunoprecipitated using 1 μg of anti-Axl AF154 (R&D Systems) together with 30 μl of protein G-Sepharose suspension for 1.5 h at 4 °C. The beads were pelleted at 1000 × *g* for 5 min at 4 °C and washed once with lysis buffer. The beads were incubated in reducing Laemmli sample buffer for 5 min at 95 °C, after which the supernatants were subjected to SDS-PAGE and Western blot, followed by probing membranes with anti-phosphotyrosine (pY99, Santa Cruz Biotechnology) and anti-Axl (H-124, Santa Cruz Biotechnology). Blots were developed and imaged as above.

To analyze Akt and ERK phosphorylation, lysates from above corresponding to 5 μg of total protein were subjected to Western blot analysis and probed with antibodies against phosphorylated and non-phosphorylated Akt (Akt (pan)) and p-Akt ((Ser-437) D93 XP), both from Cell Signaling and ERK (p44/42 MAPK (ERK1/2)) from Cell Signaling and anti-phospho-ERK1/ERK2 from R&D Systems. The blots were further probed for β-actin as a loading control.

Adhesion Molecule Expression—HAECs were grown to 90% confluence in 12-well plates and washed with PBS. PMPs (2×10^6/sample) were incubated with 0 or 250 ng/ml Gas6 in serum-free medium for 20 min at room temperature and added to the cells. The cells were incubated with the PMPs for 20 h after which they were detached using TrypLE Express (Life Technologies, Inc.) and transferred to microtiter plates containing full medium. The cells were washed once in 1% BSA in PBS and resuspended in fluorescently labeled antibodies against vascular cell adhesion protein (VCAM, FAB5649A), intercellular adhesion molecule (ICAM, BBA20), E-selectin (BBA21), or tissue factor (FAB23391A) (all from R&D Systems), diluted 1:50, and incubated for 1 h on ice in the dark. The cells were pelleted and washed once with 1% BSA in PBS, after which they were resuspended in 1.5 ml of 1% BSA in PBS and analyzed using flow cytometry (CyFlow Space, Partec).

Statistical Analysis—Data are presented as mean values with standard deviation (S.D.) of at least three separate experiments. In some cases, the error bars are too small to be seen in the graphs. Differences between groups were analyzed using one-way analysis of variance followed by Tukey's multiple comparison test, unless stated otherwise. *p* values below 0.05 were considered statistically significant.

Results

PMPs Bind Gas6 and Protein S—To generate a phenotypically homogeneous population of PMPs, we stimulated isolated human platelets with a calcium ionophore and collected released PMPs by ultracentrifugation. As PMPs are collected in one centrifugation step after platelet removal, we do not distinguish between released exosomes and MPs in this study. Upon ionophore stimulation of platelets, the cells obtained a rounded shape with abundant vesicles forming on and released off the

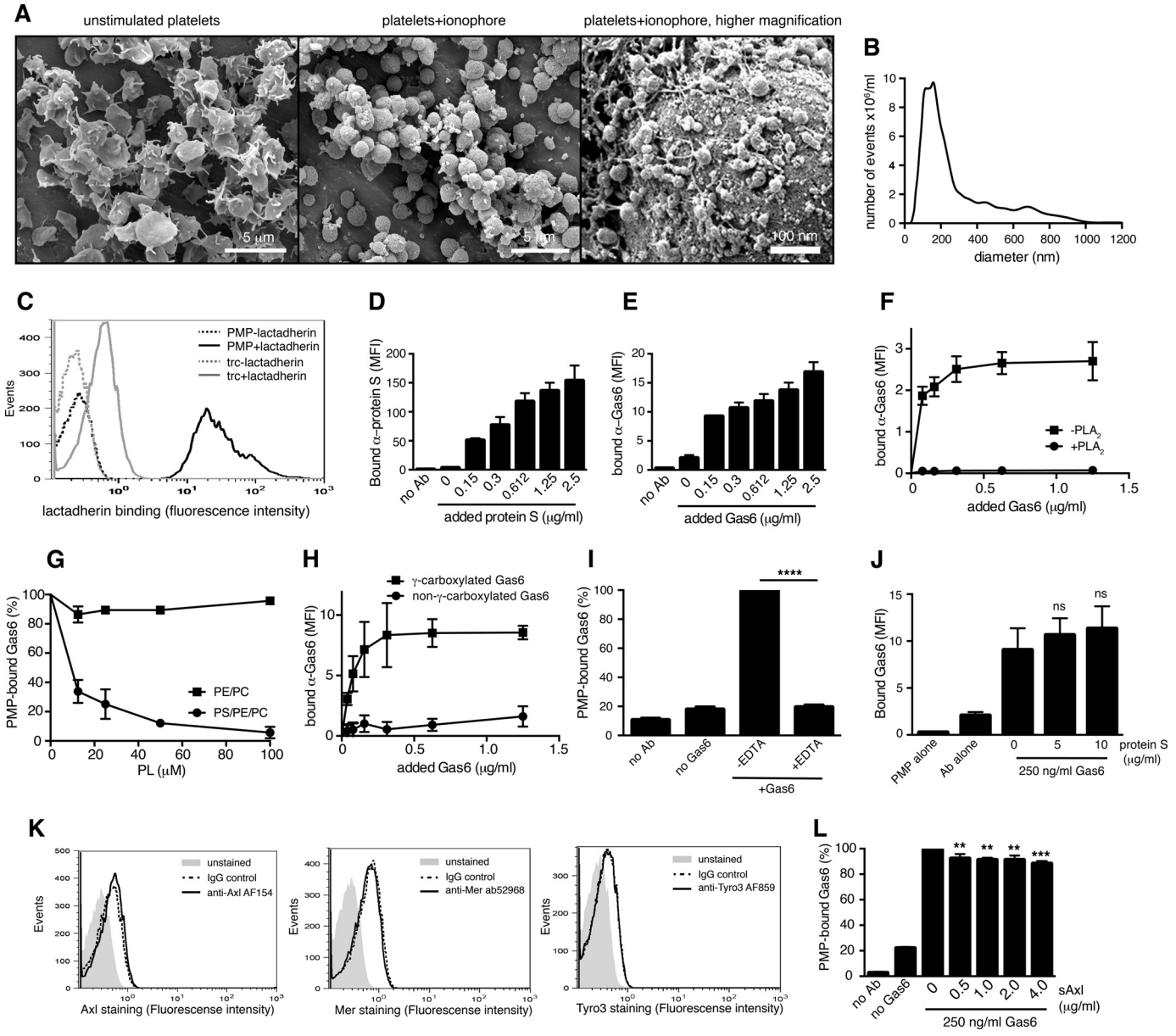

FIGURE 1. **PMPs bind Gas6 and protein S.** Scanning electron micrographs of unstimulated isolated human platelets and human platelets stimulated with a calcium ionophore to induce MP formation are shown. *A, Scale bars,* 5 μm (*left* and *middle panel*) and 100 nm (*right panel*). The MP size distribution was evaluated by nanotracking analysis and showed a mean size of just below 200 nm (*B*). PMPs were evaluated for phosphatidylserine exposure by measuring their ability to bind fluorescent lactadherin using flow cytometry (*C*). PMPs were incubated with increasing amounts of Gas6 and protein S before fluorescent antibodies (*Ab*) were added. Binding was monitored by flow cytometry (*D* and *E*). PMPs were treated with or without phospholipase A_2 (PLA_2) before Gas6 binding was evaluated by flow cytometry (*F*). Gas6 was pre-incubated with liposomes composed of PS, PE, and PC or PE and PC alone before incubation with PMPs. Gas6 binding was evaluated with flow cytometry (*G*). PMPs were incubated with γ-carboxylated (own Gas6) and non-γ-carboxylated Gas6 (RnD Gas6), and the amount of bound protein was evaluated with an antibody recognizing both Gas6 variants using flow cytometry (*H*). Gas6 was incubated with PMPs in the presence or absence of 5 mM EDTA to measure the calcium dependence of the Gas6-MP interaction (*I*). PMPs were incubated with 250 ng/ml Gas6 in the presence of increasing amounts of protein S after which fluorescent Gas6-recognizing antibodies were added. The amount of PMP-associated Gas6 was evaluated using flow cytometry (*J*). The expression of TAMs on the surface of the platelets was evaluated using flow cytometry (*K*). sAxl at increasing concentrations was pre-incubated with Gas6 before adding PMPs, and the amount of MP-bound Gas6 was evaluated using flow cytometry (*L*). Data in *D–J* and *L* are shown as mean and S.D. of three individual experiments. *C* and *K* shown representative histograms from at least three individual experiments. *ns*, not significant; **, $p < 0.01$; ***, $p < 0.001$; ****, $p < 0.0001$. *MFI*, mean fluorescent intensity.

surface (Fig. 1*A*). To estimate the size of our ionophore-induced PMPs, we analyzed them by nanotracking analysis, which demonstrated that the mean size of the particles was just below 200 nm (Fig. 1*B*), matching well the reported size of naturally occurring PMPs. A general feature of PMPs of different cellular origin is their exposure of PS on the outer membrane. Our PMPs readily exposed PS, as measured by lactadherin binding (Fig. 1*C*), further confirming their resemblance to physiological PMPs. In addition to binding protein S as has been reported earlier (48), we found that PMPs interact with Gas6 in a concentration-dependent manner (Fig. 1, *D* and *E*). As protein S has been shown to interact via its GLA domain with the exposed PS on the PMP, we evaluated whether this is the case also for Gas6. When PMPs were treated with phospho-

lipase A_2, an enzyme that hydrolyzes phospholipids into arachidonic acid and lysophospholipids, Gas6-binding was abolished, demonstrating that Gas6 interacts with phospholipids on the PMP surface (Fig. 1*F*). To confirm that the main ligand was PS, Gas6 was pre-incubated with phospholipid vesicles composed of either 80% PC and 20% PE or alternatively 60% PC, 20% PE, and 20% PS before addition to the PMPs. Only PS-containing vesicles were able to block the interaction between Gas6 and the PMPs, indicating that PS is a binding site for Gas6 on the PMPs (Fig. 1*G*). In addition, a commercially available Gas6, which has previously been shown to lack proper γ-carboxylation of the GLA domain (46), did not bind PMPs (Fig. 1*H*). EDTA blocked the Gas6-PMP interaction completely, showing that the interaction is furthermore dependent on calcium, a general feature of GLA-dependent interactions with negatively charged phospholipids (Fig. 1*I*). Despite both protein S and Gas6 binding to the exposed PS on the PMP, they did not compete for the same binding site, as protein S could not inhibit the binding of Gas6 to PMPs even at high doses (Fig. 1*J*). Previous studies have shown that both protein S and Gas6 may bind simultaneously to apoptotic cells and that neither protein S nor Gas6 binding to the apoptotic cell is disturbed by annexin V (49). Consistent with this observation, annexin V at 500-fold molar excess inhibited Gas6 from binding to PMPs only to an average of 26% and protein S from binding to PMPs to 44% (data not shown).

Earlier studies have reported conflicting results on whether human platelets themselves express TAMs. Gould *et al.* (50) demonstrated using flow cytometry that human platelets contain all three TAMs, whereas Cosemans *et al.* (51) showed that platelets contain intracellular Axl using immunoelectron microscopy. We were not, however, able to detect TAM receptors on human platelets by flow cytometry (Fig. 1*K*) or Western blot analysis (data not shown) using our in-house polyclonal antibodies or commercially available antibodies. A recent study utilizing mass spectrometry to describe the whole platelet proteome reported the presence of protein S but not Gas6 or TAM receptors in platelets (52). In this study, proteins expressed at even less than 500 copies per platelet were identified, indicating that if TAMs were present in platelets, they would indeed be expressed at a very low level. To rule out that Gas6 might bind to any Axl present on the platelet surface, we evaluated the ability of a soluble Axl (sAxl) construct comprising the extracellular domain alone to block the interaction between Gas6 and the PMPs. sAxl at a high molar overdose inhibited the binding of Gas6 to the PMPs only to ~10%, demonstrating that PMP Axl is not an important binding site for Gas6 (Fig. 1*L*). This was further confirmed by the lack of interaction of the improperly γ-carboxylated Gas6 with the PMPs (Fig. 1*H*), as the binding of Gas6 to TAMs has been shown to be normal in the absence of a functional GLA domain (53).

HUVECs and HAECs Ingest PMPs in a Gas6-Axl-dependent Manner—HUVECs have previously been shown to express TAMs, and we confirmed the presence of cell surface Axl and Mer by flow cytometry, whereas no Tyro3 expression could be detected (Fig. 2*A*). To investigate their relative abundance, the cell surface was biotinylated, after which Axl and Mer were immunoprecipitated and analyzed by Western blot for biotin (Fig. 2*B*). We found that Axl and Mer expression varied somewhat depending on the cell confluence and growth conditions, but generally their expression was in the same order of magnitude, *i.e.* none of the proteins was expressed more than 5-fold more abundantly than the other.

To elucidate whether HUVECs could ingest PMPs, PKH67-labeled PMPs were first pre-incubated with an increasing amount of Gas6, after which they were incubated with HUVECs for 1 h. Flow cytometric analysis of the cells showed a dose-dependent uptake of Gas6-coated PMPs (Fig. 2*C*). The Gas6-mediated uptake was abolished by treating the cells with Axl-targeting antibodies, whereas antibodies against Mer or Tyro3 had no effect (Fig. 2*D*).

To rule out any effect of the added fluorescent marker on the PMPs, a biotinylated preparation of PMPs was generated. Proper biotin labeling of the PMPs was verified both using flow cytometry (Fig. 2*E*) as well as Western blotting (Fig. 2*F*), which showed that several surface proteins on the PMPs were biotinylated. The strongest band around 100 kDa was used for quantification in uptake experiments. Biotinylated PMPs were incubated with HUVECs for 1 h after which their uptake was monitored by Western blot analysis of cell lysates. Only a very low uptake of PMPs by HUVECs was observed in the absence of Gas6, whereas Gas6 induced a strong, dose-dependent PMP ingestion (Fig. 2*G*). This uptake was evident already at Gas6 concentrations below 100 ng/ml, indicating that very low, physiologically relevant amounts of Gas6 are sufficient to induce PMP uptake.

Incubating the cells with an excess of unlabeled PMPs during the uptake attenuated the uptake of fluorescent PMPs, confirming the specificity of the process (Fig. 2*H*). The uptake was furthermore inhibited in the presence of EDTA, which prevents Gas6 from binding to the PMP surface (Fig. 2*I*). These results show that HUVECs can ingest PMPs in an Axl-Gas6-dependent manner.

We further evaluated the ability of primary aortic endothelial cells (HAEC) to ingest PMPs to investigate whether other types of endothelial cells display similar properties. The expression pattern of TAMs on HAECs was found to be similar to that on HUVECs (Fig. 3, *A* and *B*). Similarly to these cells, HAECs also ingested PMPs in a Gas6-dependent manner (Fig. 3*C*). Targeting cell-surface Axl with antibodies or silencing the Axl expression with siRNA abolished the uptake, as in HUVECs (Fig. 3, *D* and *E*). Importantly, non-γ-carboxylated Gas6 did not induce PMP phagocytosis even at higher concentrations (Fig. 3*G*). The amount of ingested particles increased dramatically as the incubation time was extended (Fig. 3*H*), mainly in a Gas6-dependent manner.

Gas6 Stimulates PMP Uptake Even in the Presence of Protein S—As protein S is an abundant plasma protein and was found to readily bind PMPs, we evaluated its ability to induce PMP uptake. Surprisingly, physiological amounts of protein S did not increase PMP uptake in HUVECs (Fig. 4*A*) and actually inhibited the Gas6-independent uptake in HAECs (Fig. 4*B*). This shows that different endothelial cells have different basal PMP uptake mechanisms. Correspondingly, Gas6 readily increased the PMP uptake in HUVECs even in the presence of 10 μg/ml protein S (Fig. 4*C*). In HAECs, Gas6 gave a dose-dependent

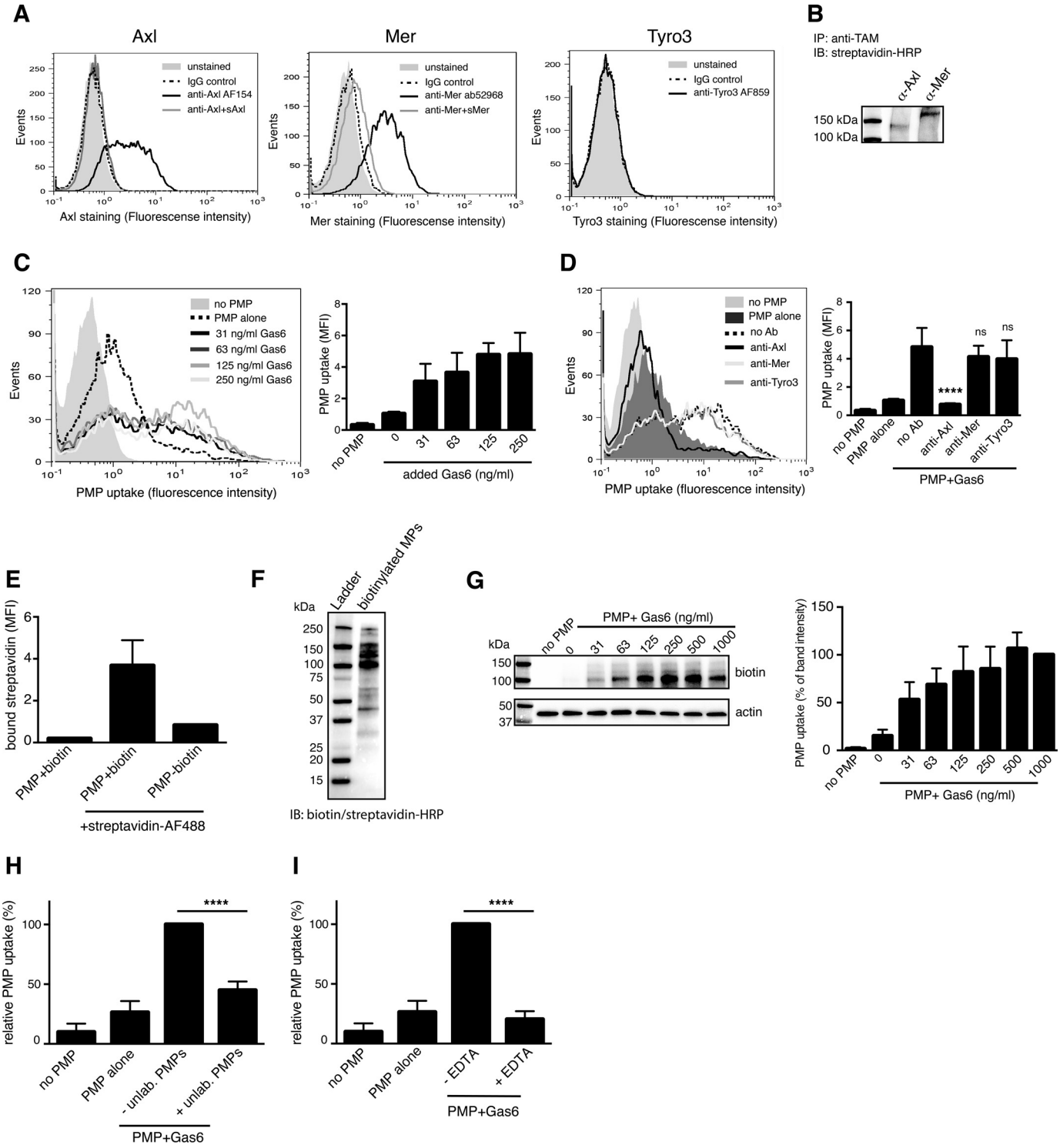

FIGURE 2. **HUVECs ingest PMPs in a Gas6-Axl-dependent manner.** TAM expression on the surface of HUVECs was evaluated using flow cytometry. Antibody specificity was verified by pre-incubating the anti-TAMs with soluble TAMs prior to addition of cells (*A*). The relative expression of Axl and Mer on the plasma membrane was measured by Western blotting after immunoprecipitation (*IP*) of Axl and Mer from cell-surface biotinylated HUVECS (*B*). *IB*, immunoblot. HUVECs were incubated with fluorescent PMPs in the presence of increasing amounts of Gas6, and uptake was monitored by flow cytometry (*C*). TAM specificity in the uptake was evaluated by incubating the cells with polyclonal antibodies against the extracellular domain of the different TAMs before and during uptake (*D*). Successful biotinylation of PMPs was measured by binding of Alexa Fluor 488-conjugated streptavidin by flow cytometry (*E*) and by Western blot analysis followed by detection with HRP-conjugated biotin-avidin complexes (*F*). Several PMP proteins were found to be biotinylated, of which the most abundant around 100 kDa was used for quantification. Biotinylated PMPs pre-incubated with increasing amounts of Gas6 were added to HUVECs cells, and after 1 h at 37 °C cells were analyzed for biotin content. A representative biotin detection by Western blot is shown to the *left* (*G*). Fluorescent PMPs were incubated with Gas6 and a double amount of unlabeled PMPs before incubating with HUVECs for 1 h. The amount of phagocytosed labeled PMPs was measured in a flow cytometer (*H*). PMPs were incubated with Gas6 in the presence or absence of 2.5 mM EDTA before adding to the cells. MP ingestion was measured as above (*I*). Data in *bar graphs* are shown as mean and S.D. of three individual experiments except for *E*, which includes two separate experiments. Other panels show representative data from at least three separate experiments. *ns*, not significant; ****, $p < 0.0001$. *MFI*, mean fluorescent intensity.

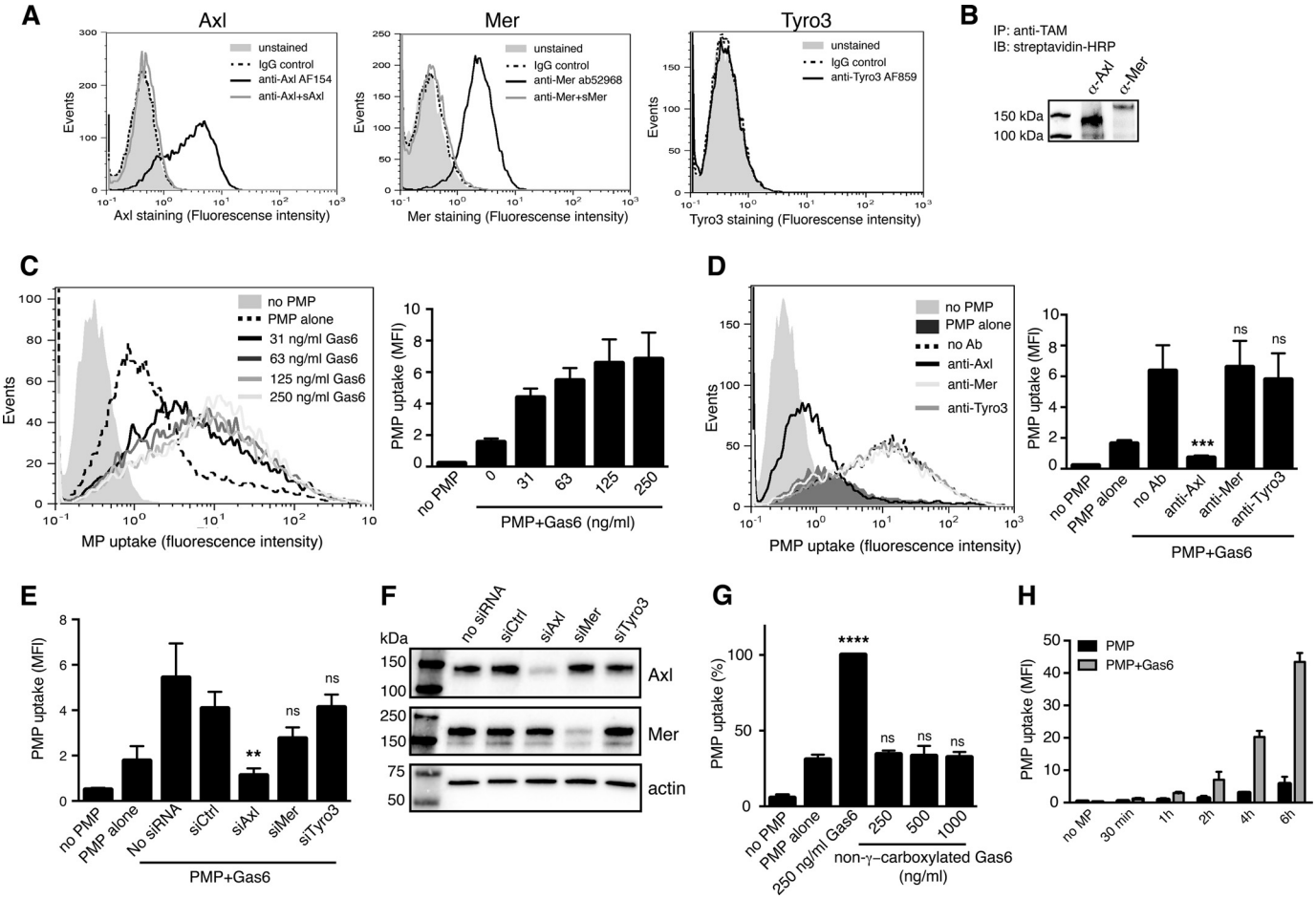

FIGURE 3. **HAECs ingest PMPs in a Gas6-Axl-dependent manner.** TAM expression was evaluated in the HAECs using flow cytometry (*A*). Relative expression of Axl and Mer at the cell surface was evaluated by Western blotting of immunoprecipitated TAMs after cell surface biotinylation (*B*). Fluorescent PMPs were incubated with Gas6 and fed to HAECs for 1 h at 37 °C. PMP phagocytosis was measured by flow cytometry (*C*). The TAM dependence of the uptake was evaluated by introducing TAM-targeting antibodies during the uptake (*D*) or by treating the HAECs with siRNA targeting the different TAMs (*E*). The knockdown efficiency of the TAM siRNA treatment is shown in *F*. Fluorescent PMPs were incubated with recombinant in-house purified Gas6 or commercially available non-γ-carboxylated Gas6 before incubation with HAECs (*G*). Uptake was measured as described in *D*. Fluorescent PMPs with or without Gas6 were incubated with HAECs for increasing times at 37 °C to measure the time dependence of the uptake (*H*). Uptake was measured using flow cytometry as described in *E*. Data in *bar graphs* are shown as mean and S.D. of three individual experiments. Other panels show representative data from at least three separate experiments. *ns*, not significant; **, $p < 0.01$; ***, $p < 0.001$; ****, $p < 0.0001$.

stimulation of uptake even in the presence of protein S. However, the total uptake signal was relatively low due to the protein S-dependent blockage of the basal uptake (Fig. 4*D*). When the uptake experiment was carried out on ice, thereby preventing active ingestion, and without the trypsinization that we used to detach cell surface-bound particles, hardly any binding of PMPs to the HAECs could be observed, even in the presence of Gas6 or protein S (data not shown). This suggests that other mechanisms are responsible for the initial interaction of the PMP with the cell, whereas Gas6 mainly potentiates the actual ingestion process. Consistent with the observation of annexin V only partially inhibiting the binding of Gas6 to the PMPs, annexin V inhibited Gas6-mediated PMP uptake in HUVEC to ~50% but did not interfere with the basal uptake (Fig. 4*E*).

sAxl Interferes with Uptake Depending on the Cell Type—Circulating Gas6 has been shown to be in complex with soluble Axl (41), which might be a result of proteolytic Axl release from the cell surface upon activation by Gas6 (53). The amount of free Gas6 seems to be the limiting factor determining the amount of formed complexes, as there is a molar excess of soluble Axl in plasma as compared with Gas6 (41). However, cells of the vasculature have been shown to produce Gas6 (54), which might result in free Gas6 molecules locally around the vascular wall. Soluble Axl is found in the circulation in healthy humans at concentrations ranging from 14 to 105 ng/ml, with a mean concentration of 42 ng/ml (41). Interestingly, soluble Axl at concentrations up to 500 ng/ml caused only a slight decrease in the Gas6-dependent PMP uptake in HAECs, whereas in HUVECs sAxl had a more pronounced inhibitory effect (Fig. 4, *F* and *G*) showing that the presence of physiological sAxl concentrations do not prevent PMP ingestion.

PMPs Are Actively Internalized and Localize Around Nuclei—Using confocal microscopy, we could see that the ingested Gas6-coated PMPs were properly internalized in the HAECs as opposed to merely bound to the cell surface, and they accumulated around the nucleus (Fig. 5*A*).

To further investigate the internalization process, we studied the uptake of biotinylated PMPs in HAEC cells by transmission electron microscopy where PMPs were visualized using an avidin-gold conjugate (Fig. 5*B*). PMPs of different sizes were found

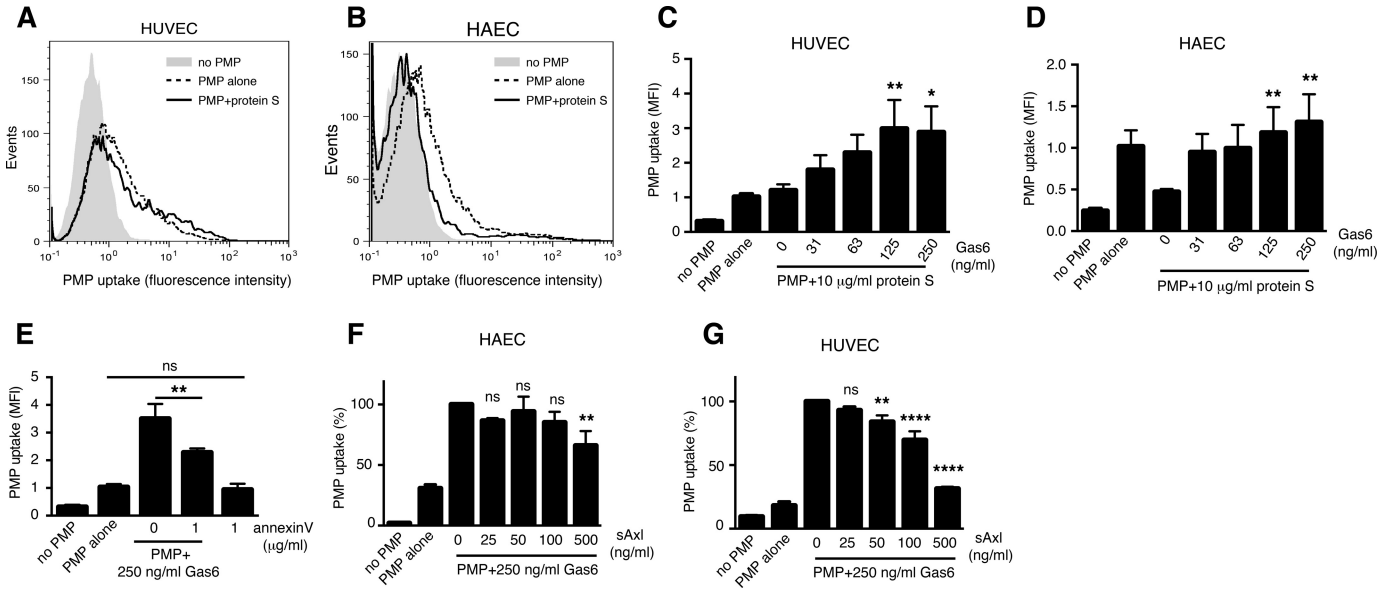

FIGURE 4. **Protein S blocks basal PMP uptake only in HAECs.** Fluorescent PMPs pre-treated with or without 10 μg/ml protein S were incubated for 1 h with HUVECs (*A*) or HAECs (*B*). PMP uptake was measured by flow cytometry. The combinatory effect of protein S and Gas6 on PMP uptake was measured by incubating fluorescent PMPs with 10 μg/ml protein S in the presence of increasing amounts of Gas6 before incubating the PMPs with HUVECs (*C*) or HAECs (*D*). Fluorescent PMPs were incubated with 250 ng/ml Gas6 and 0 or 1 μg/ml annexin V before feeding them to HUVECs (*E*). PMPs were incubated with 250 ng/ml Gas6 and increasing amounts of sAxl before uptake was evaluated in HAECs (*F*) and HUVECs (*G*). Data show the mean and S.D. of at least three separate experiments except for *A* and *B*, which show representative histograms from three individual experiments. *ns*, not significant; *, $p < 0.05$; **, $p < 0.001$; ****, $p < 0.0001$. *MFI*, mean fluorescent intensity.

inside the cells both freely in the cytoplasm as well as in structures resembling endosomal vesicles. Whether these were vesicles taken up by two distinct pathways or merely showed the same process at different time points remains to be elucidated.

The Gas6-dependent PMP phagocytosis in HAECs was an active process, as inhibition of cytoskeletal rearrangement with cytochalasin D or nocodazole prevented PMP uptake (Fig. 5*C*). At the used concentrations, neither cytochalasin D nor nocodazole induced endothelial exposure of the apoptosis marker PS, as measured by annexin-V staining. Furthermore, the binding of Gas6 to the PMPs was not inhibited in the presence of either chemical (data not shown).

PMP-bound Gas6 Phosphorylates Axl—Axl activation depends on phosphorylation of its intracellular kinase domain. Gas6 on its own is able to trigger Axl phosphorylation, but recent studies have suggested that the presence of PS-exposing membranes increases the potential of Gas6 to phosphorylate Axl (53). We found that PMPs on their own did not phosphorylate Axl, but binding of Gas6 to the PMPs potentiated the ability of Gas6 to activate Axl (Fig. 6*A*). Axl activation by Gas6 has been shown to induce downstream activation or Akt and ERK1/2 MAPKs in several cell lines. Gas6 stimulation of HAECs induced Akt phosphorylation, which was further increased by the presence of PMPs (Fig. 6*B*). However, PMPs on their own also induced a certain amount of Akt phosphorylation in HAECs. The PMPs also induced a low amount of ERK1/2 phosphorylation (Fig. 6*C*), whereas Gas6 had no effect on ERK1/2 activation in these cells. This shows that PMP-bound Gas6 may induce differential Axl signaling in the endothelium compared with circulating Gas6 or at least affect the intensity of the stimulation. Addition of an Axl kinase inhibitor (R428) prevented Gas6-dependent uptake of fluorescent PMPs in HAECs, confirming that the observed Axl phosphorylation is necessary to trigger ingestion (Fig. 6*D*).

Thrombin/Collagen-generated PMPs Are Ingested Similarly to Ionophore-generated PMPs—PMPs generated by ionophore stimulation may have a different phenotype from physiological PMPs generated in the circulation, and differences in the size and proteome of formed PMPs have been described when platelets were stimulated with an ionophore or a combination of thrombin and collagen (3). To elucidate whether the uptake we observe is dependent on the mechanism by which we induce PMP formation, we stimulated purified human platelets with a combination of thrombin and collagen and isolated and labeled released PMPs (TC-PMPs) with the same techniques that were used for the ionophore PMPs. When analyzed by electron microscopy, the thrombin- and collagen-stimulated platelets showed signs of typical platelet activation with pseudopod formation and aggregation, in contrast to the ionophore-activated platelets (Fig. 7*A*). The size of the TC-PMPs was more heterogeneous than that of the ionophore PMPs, as evaluated by nanotracking analysis (Fig. 7*B*). They also exposed slightly lower levels of PS than ionophore-induced PMPs (Fig. 7*C*), which was further reflected in a lower protein S and Gas6 binding (Fig. 7, *D* and *E*). Nevertheless, TC-PMPs were readily phagocytosed by HAECs in a Gas6-dependent manner, whereas protein S, as expected, did not stimulate uptake (Fig. 7*F*). This shows that also PMPs generated in a more physiological manner are taken up in primary human endothelium in a Gas6-dependent way.

Erythrocyte MPs and THP-1 MPs Are Less Dependent on Gas6 for Uptake in HAEC—We further wanted to study whether MPs derived from other host cells could be taken up in HAECs via Gas6 and TAMs. Aged erythrocytes have been

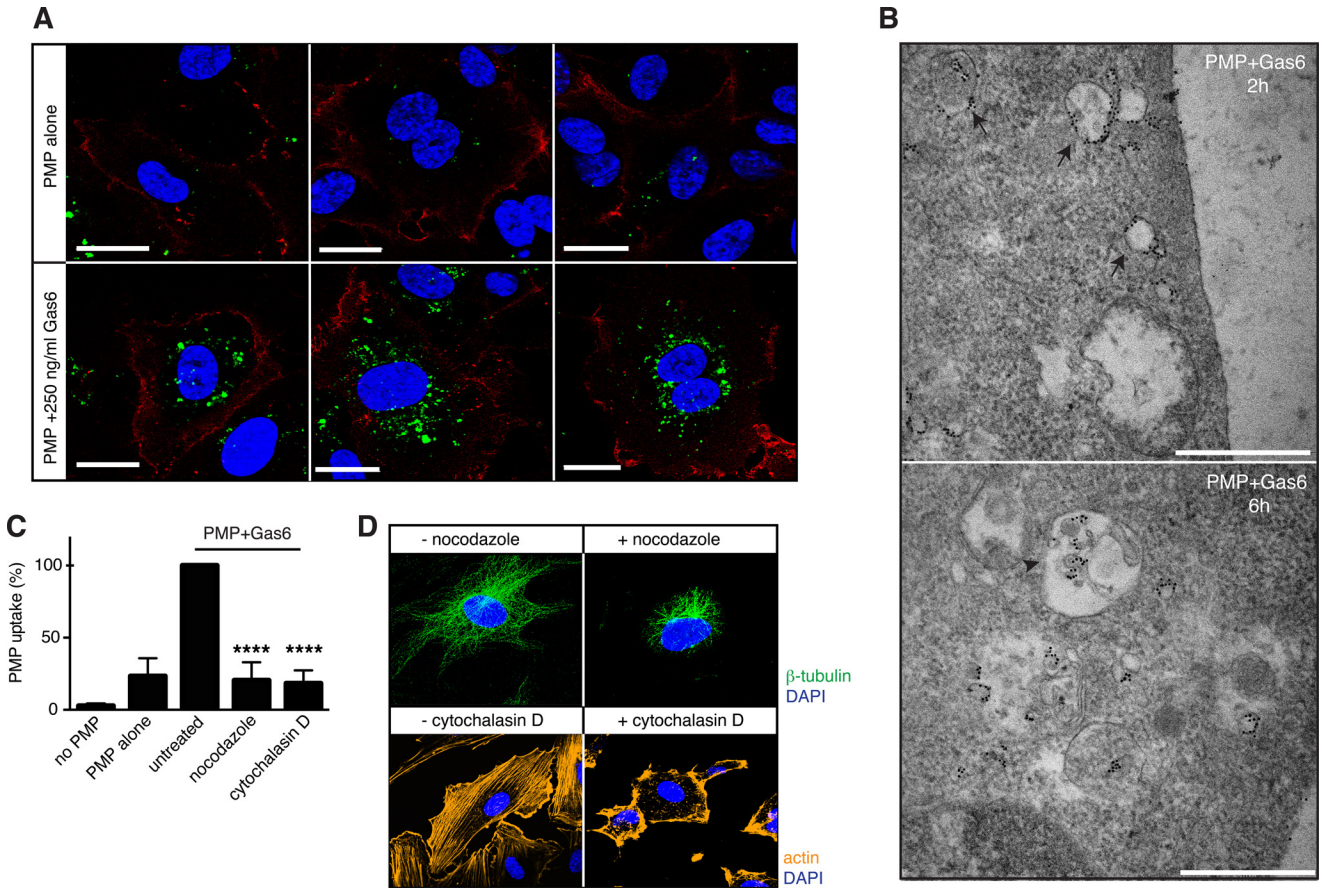

FIGURE 5. **PMPs are actively ingested and transported to the nuclear vicinity.** HAECs were grown on coverslips and incubated with fluorescent PMPs in the presence and absence of Gas6 for 4 h. Cells were fixed, and the cell membrane was stained with an antibody against CD31, after which uptake was evaluated using confocal microscopy. CD31 is shown in *red*; PMPs are shown in *green*, and the nuclei are shown in *blue* (*A*). Uptake of Gas6-coated biotinylated PMPs was investigated using transmission electron microscopy. Cells were stained with an avidin-gold conjugate to visualize PMPs. *Arrows* point to PMPs moving freely in the cell and *arrowheads* to PMPs enclosed in endosome-like compartments (*B*). *Scale bars,* 20 μm (*A*) and 500 nm (*B*). HAECs were treated with cytochalasin D or nocodazole prior to and during uptake of fluorescent PMPs in the presence and absence of Gas6. Uptake was measured by flow cytometry (*C*). Successful disruption of the microtubule and the actin networks was verified by staining the cells with anti-β-tubulin and fluorescent phalloidin (*D*). Data in *A* show representative images from at least three individual experiments, and *C* shows the mean and S.D. of three separate experiments. *B* shows two out of several representative images from one uptake experiment. ****, $p < 0.0001$.

shown to be ingested in angiogenic HUVECs in a manner dependent on lactadherin (55), and eryMPs are known to bind protein S (56). We therefore evaluated whether Gas6 could interact with eryMPs and induce their uptake in HAECs. The eryMPs were generated by stimulation of purified human erythrocytes with a calcium ionophore and isolated by ultracentrifugation as the PMPs. They exposed PS on their surface as shown by their ability to bind lactadherin (Fig. 7*G*) and protein S (Fig. 7*H*). In contrast, Gas6 showed only a very weak binding to isolated eryMPs (Fig. 7*I*). PKH67-labeled eryMPs were readily phagocytosed by HAECs even in the absence of Gas6, but the uptake was significantly increased when Gas6 was present (Fig. 7*J*). This shows that even minor amounts of Gas6 on the surface of the eryMP are sufficient to promote uptake. This may indicate that other proteins regulate the docking process of the eryMP to the cell surface, whereas Gas6 triggers the actual ingestion process.

THP-1 MPs have also shown to be phagocytosed by endothelial cells (57). We therefore generated THP-1 MPs by LPS stimulation, which generated PS-positive particles (Fig. 7*K*) that in addition had the ability to bind protein S and Gas6 (Fig. 7, *L* and *M*). HAECs were able to phagocytose THP-1 MPs, an effect which was slightly, but not significantly, increased in the presence of Gas6 (Fig. 7*N*). Therefore, it seems that uptake mechanisms are slightly different both for MPs from different sources as well as in different endothelial cells.

Inflammatory Regulation by PMPs—Several reports have shown that PMPs may have pro-inflammatory effects on the endothelium, among others, by up-regulating the expression of adhesion molecules such as intercellular adhesion molecule (ICAM) (12, 13) as well as cytokine secretion. When incubating HAECs for 20 h with PMPs, we saw a slight but significant increase in ICAM expression, and this was further increased in the presence of PMP-bound Gas6 (Fig. 8). PMPs also induced the expression of E-selectin, again a feature, which was augmented in the presence of Gas6 (Fig. 8). However, only negligible amounts of VCAM and tissue factor were expressed on the HAECs after 20 h of MP stimulation. This confirms that PMPs do have a weakly pro-inflammatory phenotype, which seems to be increased when their uptake is promoted.

Circulating PMPs in Gas6$^{-/-}$ Mice—As Gas6 was shown to be an important mediator of PMP uptake in cultured human endothelium, we investigated whether the same was true *in vivo* in mice. We therefore compared the levels of circulating CD41-

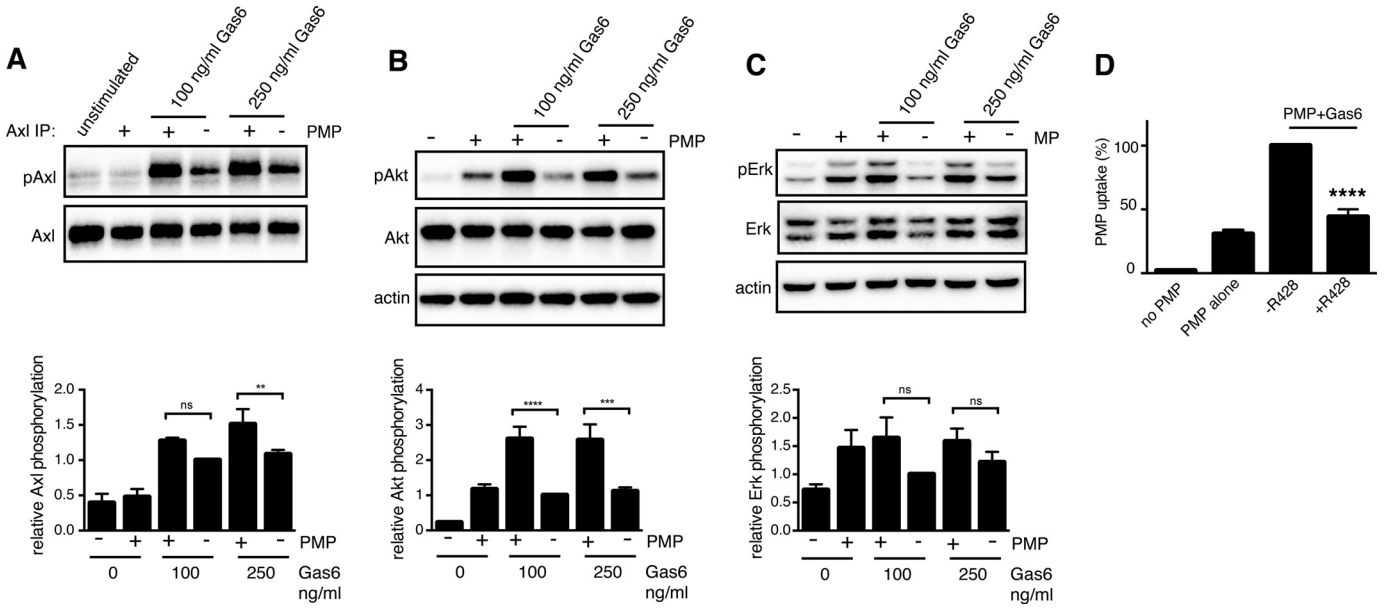

FIGURE 6. **PMP-bound Gas6 activates Axl better than free Gas6.** HAECs were stimulated with PMPs alone or PMPs together with Gas6 for 15 min, after which cells were lysed. Axl phosphorylation was measured by Western blot in samples after immunoprecipitation (*IP*) with Axl-specific antibodies. Total Axl in immunoprecipitated samples served as loading control (*A*). The level of Akt (*B*) and ERK (*C*) phosphorylation upon stimulation with PMPs in the presence or absence of Gas6 was measured in cell lysates. Cells were treated with an Axl kinase inhibitor (R428) for 15 min prior to and during uptake of fluorescent PMPs. The level of uptake was measured by flow cytometry (*D*). Data show the mean and S.D. of three separate experiments. *ns,* not significant; **, $p < 0.01$; ***, $p < 0.001$; ****, $p < 0.0001$.

positive PMPs in platelet-poor plasma of *Gas6*$^{-/-}$ and *Gas6*$^{+/+}$ mice. We found no significant differences in the amount of circulating CD41^{+}PS^{+} PMPs under basal conditions in the mice (*Gas6*$^{-/-}$, mean 4059 PMP/μl; *Gas6*$^{+/+}$, mean 4028 PMP/μl) nor in the amount of CD41 single-positive PMPs (*Gas6*$^{-/-}$, mean 532 PMP/μl; *Gas6*$^{+/+}$, mean 383 PMP/μl) (Fig. 9*A*). No significant differences were observed either when all PS^{+} MPs, *i.e.* not only the CD41-positive events, were analyzed (*Gas6*$^{-/-}$, mean 13417 MP/μl; *Gas6*$^{+/+}$, mean 11303 MP/μl), showing that in general the levels of circulating MPs of different origins were not altered in *Gas6*$^{-/-}$ mice (Fig. 9*B*). Circulating MP levels were not affected by age; however, in both *Gas6*$^{-/-}$ and *Gas6*$^{+/+}$ mice, levels of PMPs as well as MPs in general were higher in males than females.

Discussion

Platelet MPs, which represent a large portion of circulating MPs, expose high amounts of PS, are highly pro-coagulant, and have been suggested to contribute to thrombotic events. Despite their possibly harmful properties, little is still known about both the physiological function of PMPs and their mode of clearance. Here, we show that PMPs are readily ingested in primary human endothelial cells in a Gas6- and Axl-dependent manner. This uptake mechanism was not restricted to PMPs as also eryMPs were ingested in a Gas6-dependent manner. Despite the high abundance of the Gas6 homologue protein S in circulation and the ability of protein S to interact with Mer and Tyro3, exclusively Gas6 together with Axl were able to mediate MP phagocytosis in endothelium. This was not due to a substantial overexpression of Axl compared with Mer in the cells, but most likely reflects the higher affinity that Gas6 displays for Axl than for Mer. However, it has been demonstrated that most of the circulating Gas6 is bound to soluble Axl, which could argue that circulating Gas6 is inactive (41). Interestingly, we observed only a weak inhibition of PMP uptake in HAECs when Gas6 was pre-incubated with sAxl, whereas the inhibition was stronger in HUVECs. It is possible that Axl is glycosylated differently in various cells or associated with different receptor complexes altering its affinity for Gas6. Axl expressed in HAEC may form a stronger complex with Gas6 than the recombinant sAxl, thus promoting uptake. The cellular source of circulating sAxl may therefore be crucial for its ability to interfere with Axl/Gas6 signaling in different tissues. Alternatively, sAxl-Gas6-PMP complexes can possibly be recognized by Axl on HAECs, thereby promoting the association of PMPs to the cell surface. In this case, other PS-recognizing receptors could stimulate the actual ingestion process. Both endothelial cells and vascular smooth muscle cells produce and secrete Gas6 (54, 58), thereby possibly increasing the Gas6 concentration locally at the vessel wall. Moreover, the interaction between Gas6 and PS-exposing apoptotic cells has been shown to occur within seconds (49), which might also be the case for the Gas6-PMP interaction. This would allow locally produced, newly released free Gas6 to complex with PMPs and trigger their uptake. The contribution of endothelial Gas6 for PMP uptake *in vivo* is, however, still unclear.

Protein S was found to inhibit Gas6-independent PMP uptake in HAECs but not in HUVECs, and antibodies targeting the protein S GLA domain abolished the inhibitory effect (data not shown), which indicates that protein S needs to associate with PS on the PMP to exert its inhibitory effect. It is likely that protein S can compete out the binding of other MP-opsonizing PS ligands that mediate PMP uptake specifically in HAECs but not HUVECs. We also demonstrated that despite both protein S and Gas6 binding to PS on the PMP, neither of the molecules

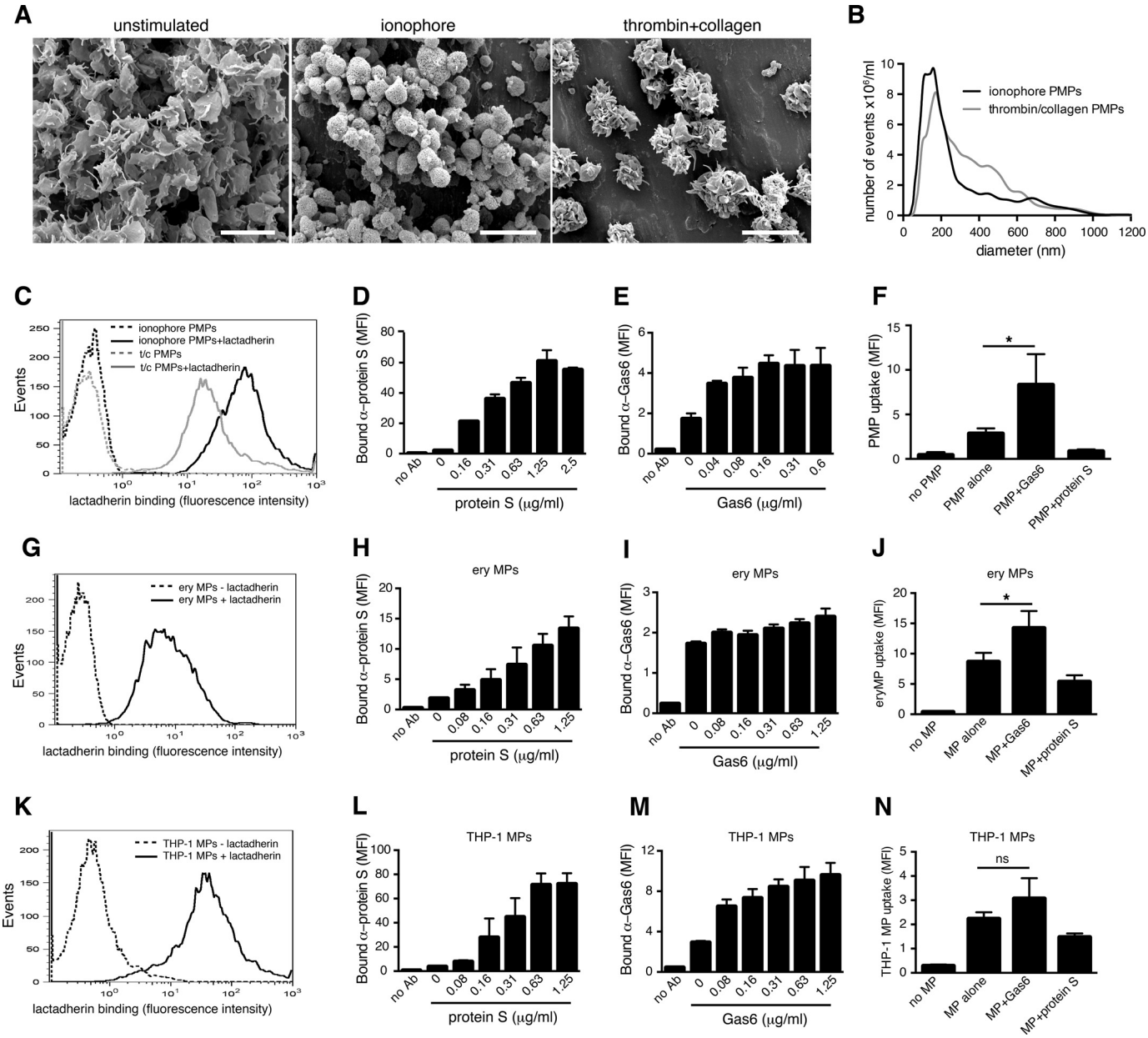

FIGURE 7. **PMPs generated with thrombin and collagen are ingested equally well as ionophore-generated PMPs.** The appearance of platelets stimulated with thrombin/collagen was visualized with scanning electron microscopy, showing a more typical platelet activation phenotype compared with ionophore-stimulated platelets (*A*). *Scale bars* denote 5 μm. The size of thrombin/collagen PMPs was compared with that of ionophore PMPs by nanotracking analysis and showed a more heterogeneous size distribution (*B*). The amount of PS exposure on the different PMPs was measured by evaluating lactadherin binding by flow cytometry (*C*). Binding of protein S (*D*) and Gas6 (*E*) to thrombin/collagen PMPs was evaluated by flow cytometry. The uptake of fluorescent thrombin/collagen PMPs into HAECs was measured in the presence of Gas6 and protein S using flow cytometry (*F*). Erythrocyte MPs were measured for their ability to bind lactadherin (*G*), protein S (*H*), and Gas6 (*I*). The influence of Gas6 and protein S on the uptake of fluorescent erythrocyte MPs in HAECs was measured by flow cytometry (*J*). Lactadherin (*K*), protein S (*L*), and Gas6 (*M*) binding to THP-1 MPs generated by LPS stimulation was measured using flow cytometry. The ability of Gas6 and protein S to modulate the uptake of fluorescent THP-1 MPs in HAECs was measured as above (*N*). Data show the mean and S.D. of at least three separate experiments, except for histograms, which are representative for three experiments. *ns,* not significant; *, $p < 0.05$. *MFI*, mean fluorescent intensity.

competed with each other for the same binding site, and annexin V could only partially compete out protein S and Gas6 from the PMP. This indicates that membrane microdomains, and not general PS exposure, are important for the selective association of PS ligands.

A previous study demonstrated Del-1-dependent PMP uptake by HUVECs already within 30 min of PMP exposure and also showed the importance of Del-1 for PMP uptake in lung and liver endothelium *in vivo* in mice (20). As we observed that the basal uptake mechanism in the absence of Gas6 differs between different types of endothelium, it is possible that uptake mechanisms differ in different organs. PMPs ingested in a Del-1-dependent manner accumulated to one side in the cell periphery, whereas Gas6-Axl-mediated uptake showed a clear transport of PMPs to the immediate vicinity of the nucleus. This suggests that the uptake processes engage different pathways and may direct the PMPs to different intracellular processing, alternatively the cellular location differs upon increas-

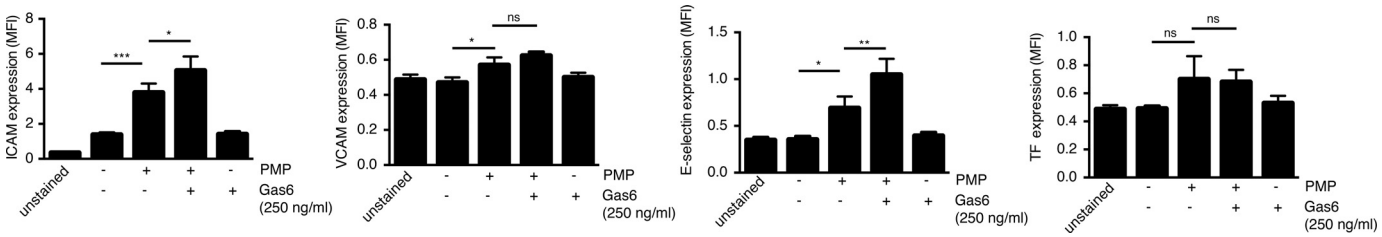

FIGURE 8. **Gas6 increases PMP-induced ICAM and E-selectin expression.** HAECs were incubated with PMPs in the presence or absence of Gas6 for 20 h after which their cell-surface expression of adhesion molecules was evaluated by flow cytometry. Data show the mean and S.D. of three separate experiments. *ns*, not significant; *, $p < 0.05$; **, $p < 0.01$; ***, $p < 0.001$.

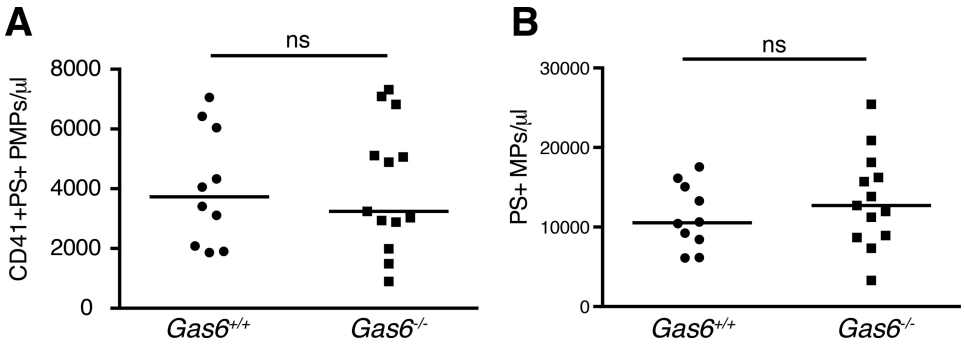

FIGURE 9. **Basal levels of circulating PMPs are not altered in *Gas6*$^{-/-}$ mice compared with *Gas6*$^{+/+}$ mice.** Levels of circulating CD41$^+$PS$^+$ PMPs (*A*) or PS$^+$ MPs (*B*) were measured in *Gas6*$^{-/-}$ ($n = 13$) and *Gas6*$^{+/+}$ ($n = 10$) mice using flow cytometry. *Horizontal bars* denote the median. Statistical analysis of differences between the groups was carried out using a Mann-Whitney test. *ns,* not significant.

ing the uptake time, as we in our study visualized the cells after 4 h of uptake. Furthermore, Del-1-mediated phagocytosis was restricted to larger PMPs sedimented at 20,000 × *g*. In this study, we did not differentiate between big and small PMPs or PMPs and platelet-derived exosomes, and it is possible that Gas6-mediated uptake is restricted to a subpopulation of released vesicles. Brain endothelial cells were also shown to phagocytose PMPs in an active process depending on calcium, which was increased in the presence of heat-inactivated serum. Brain endothelial cells have been shown to express all three TAMs, which may interact with Gas6 and protein S (59, 60). Any of these receptors may potentially be responsible for PMP uptake in brain endothelium.

Axl-mediated phagocytosis has previously been described to occur mainly in dendritic cells (25, 61) and specifically under pro-inflammatory conditions (62), whereas Mer in both circulating and tissue-resident macrophages was suggested to contribute to homeostatic apoptotic clearance under tolerogenic settings. As the PMPs represent a large part of circulating MPs even under basal conditions, their phagocytic uptake could be expected to occur in a constantly ongoing manner resembling homeostatic Mer-dependent phagocytosis. As this process in endothelium was independent of Mer, TAM-dependent phagocytic processes are likely to be differentially regulated in different tissues. Whether TAMs expressed on macrophages mediate uptake of PMPs is, however, still unknown.

Interestingly, we did not observe any differences in the basal levels of circulating MPs or PMPs in Gas6-deficient mice. However, we cannot exclude that different pathological conditions known to increase the release of cellular microparticles, such as metastatic cancer, thromboembolism, or severe inflammation, might induce elevated circulating MP levels in *Gas6*$^{-/-}$ mice compared with *Gas6*$^{+/+}$ mice. The uptake process may additionally be different in mice than in humans, as all cellular experiments we carried out were performed with isolated human cells and proteins. Despite extensive literature describing Axl expression in human endothelium, only a few reports have been published on the presence of Axl in murine endothelium (63, 64). However, several studies have demonstrated Gas6-mediated responses in murine endothelium. As the TAMs are the only known receptors for Gas6, it is therefore likely that members of this receptor family are expressed also in murine endothelium. Furthermore, it is likely that overlapping mechanisms for PMP removal exists, which will compensate for the loss of any single one of them. It is possible that Del-1 may mediate uptake of PMPs in endothelium in the absence of Gas6; alternatively, endothelial uptake is replaced by phagocytosis in macrophages and neutrophils. A change in uptake mechanism may in addition alter the biological impact of released PMPs. Another explanation may be that endothelial uptake of PMPs is not the predominant mechanism to clear the bulk of released PMPs from the circulation, but it may serve a specific function in regulation of endothelial responses. Such a role has been shown among others in the delivery of functional Ago2-miR-223 complexes from PMPs to HUVECs, which thereby regulate endogenous gene expression in the endothelium (22). Therefore, eliminating Gas6 would not alter the levels of circulating PMPs, as the vast majority of them would be taken up in other cells and tissues. *Gas6*$^{-/-}$ mice have been shown to have slightly altered platelet responses (40), and hence, we cannot exclude the possibility that platelets from *Gas6*$^{-/-}$ mice display reduced abilities to form PMPs. This might contribute to the decreased thrombogenicity observed in the mice, both by altering directly the initiation of coagulation as well as decreasing endothelial responses. Under basal conditions, there was no difference in the proportion of CD41$^+$

PMPs in relation to the total MP population between $Gas6^{-/-}$ and $Gas6^{+/+}$ mice (34% in $Gas6^{-/-}$ and 38% in $Gas6^{+/+}$); however, this should be further studied in detail upon platelet-activating stimuli.

In conclusion, we now show the following: 1) Gas6 interacts with platelet derived MPs, and 2) endothelial Axl can function as a phagocytic receptor. Whether this ability is limited to the uptake of MPs or whether PS-exposing apoptotic bodies are similarly ingested remains to be answered. However, this expands our knowledge on the function of both TAMs and their ligands in the vasculature and may provide valuable insights as to how platelets interact with the vessel wall. In this light it will be intriguing to unveil the purpose and destination of ingested particles, whether they are a means of transportation of genetic material into target cells or whether they are transported further into underlying tissues.

Author Contributions—K. E. H. participated in study design, performed experiments, analyzed the data, and wrote the manuscript. S. T. performed experiments and analyzed the data. M. M. performed electron microscopy. S. C. and R. P. performed experiments on mice. A. A-S. provided valuable reagents. B. D. participated in study design and supervised the study. All authors read and approved the final manuscript.

Acknowledgments—We thank Maria Baumgarten for technical assistance regarding electron microscopy and Eva Norström regarding flow cytometric analysis of microparticles.

References

1. Sinauridze, E. I., Kireev, D. A., Popenko, N. Y., Pichugin, A. V., Panteleev, M. A., Krymskaya, O. V., and Ataullakhanov, F. I. (2007) Platelet microparticle membranes have 50- to 100-fold higher specific procoagulant activity than activated platelets. *Thromb. Haemost.* **97,** 425–434
2. Somajo, S., Koshiar, R. L., Norström, E., and Dahlbäck, B. (2014) Protein S and factor V in regulation of coagulation on platelet microparticles by activated protein C. *Thromb. Res.* **134,** 144–152
3. Aatonen, M. T., Öhman, T., Nyman, T. A., Laitinen, S., Grönholm, M., and Siljander, P. R. (2014) Isolation and characterization of platelet-derived extracellular vesicles. *J. Extracell. Vesicles* **3,** 24692
4. Rank, A., Nieuwland, R., Crispin, A., Grützner, S., Iberer, M., Toth, B., and Pihusch, R. (2011) Clearance of platelet microparticles *in vivo*. *Platelets* **22,** 111–116
5. Flaumenhaft, R., Dilks, J. R., Richardson, J., Alden, E., Patel-Hett, S. R., Battinelli, E., Klement, G. L., Sola-Visner, M., and Italiano, J. E., Jr. (2009) Megakaryocyte-derived microparticles: direct visualization and distinction from platelet-derived microparticles. *Blood* **113,** 1112–1121
6. Berckmans, R. J., Nieuwland, R., Böing, A. N., Romijn, F. P., Hack, C. E., and Sturk, A. (2001) Cell-derived microparticles circulate in healthy humans and support low grade thrombin generation. *Thromb. Haemost.* **85,** 639–646
7. Horstman, L. L., and Ahn, Y. S. (1999) Platelet microparticles: a wide-angle perspective. *Crit. Rev. Oncol. Hematol.* **30,** 111–142
8. Arraud, N., Linares, R., Tan, S., Gounou, C., Pasquet, J. M., Mornet, S., and Brisson, A. R. (2014) Extracellular vesicles from blood plasma: determination of their morphology, size, phenotype and concentration. *J. Thromb. Haemost.* **12,** 614–627
9. Italiano, J. E., Jr., Mairuhu, A. T., and Flaumenhaft, R. (2010) Clinical relevance of microparticles from platelets and megakaryocytes. *Curr. Opin. Hematol.* **17,** 578–584
10. Piccin, A., Murphy, W. G., and Smith, O. P. (2007) Circulating microparticles: pathophysiology and clinical implications. *Blood Rev.* **21,** 157–171
11. Boilard, E., Nigrovic, P. A., Larabee, K., Watts, G. F., Coblyn, J. S., Weinblatt, M. E., Massarotti, E. M., Remold-O'Donnell, E., Farndale, R. W., Ware, J., and Lee, D. M. (2010) Platelets amplify inflammation in arthritis via collagen-dependent microparticle production. *Science* **327,** 580–583
12. Barry, O. P., Praticò, D., Savani, R. C., and FitzGerald, G. A. (1998) Modulation of monocyte-endothelial cell interactions by platelet microparticles. *J. Clin. Invest.* **102,** 136–144
13. Nomura, S., Tandon, N. N., Nakamura, T., Cone, J., Fukuhara, S., and Kambayashi, J. (2001) High-shear-stress-induced activation of platelets and microparticles enhances expression of cell adhesion molecules in THP-1 and endothelial cells. *Atherosclerosis* **158,** 277–287
14. Mause, S. F., von Hundelshausen, P., Zernecke, A., Koenen, R. R., and Weber, C. (2005) Platelet microparticles: a transcellular delivery system for RANTES promoting monocyte recruitment on endothelium. *Arterioscler. Thromb. Vasc. Biol.* **25,** 1512–1518
15. Sadallah, S., Eken, C., Martin, P. J., and Schifferli, J. A. (2011) Microparticles (ectosomes) shed by stored human platelets downregulate macrophages and modify the development of dendritic cells. *J. Immunol.* **186,** 6543–6552
16. Sadallah, S., Amicarella, F., Eken, C., Iezzi, G., and Schifferli, J. A. (2014) Ectosomes released by platelets induce differentiation of CD4+T cells into T regulatory cells. *Thromb. Haemost.* **112,** 1219–1229
17. Rand, M. L., Wang, H., Bang, K. W., Packham, M. A., and Freedman, J. (2006) Rapid clearance of procoagulant platelet-derived microparticles from the circulation of rabbits. *J. Thromb. Haemost.* **4,** 1621–1623
18. Dasgupta, S. K., Abdel-Monem, H., Niravath, P., Le, A., Bellera, R. V., Langlois, K., Nagata, S., Rumbaut, R. E., and Thiagarajan, P. (2009) Lactadherin and clearance of platelet-derived microvesicles. *Blood* **113,** 1332–1339
19. Abdel-Monem, H., Dasgupta, S. K., Le, A., Prakasam, A., and Thiagarajan, P. (2010) Phagocytosis of platelet microvesicles and β2- glycoprotein I. *Thromb. Haemost.* **104,** 335–341
20. Dasgupta, S. K., Le, A., Chavakis, T., Rumbaut, R. E., and Thiagarajan, P. (2012) Developmental endothelial locus-1 (Del-1) mediates clearance of platelet microparticles by the endothelium. *Circulation* **125,** 1664–1672
21. Faille, D., El-Assaad, F., Mitchell, A. J., Alessi, M. C., Chimini, G., Fusai, T., Grau, G. E., and Combes, V. (2012) Endocytosis and intracellular processing of platelet microparticles by brain endothelial cells. *J. Cell. Mol. Med.* **16,** 1731–1738
22. Laffont, B., Corduan, A., Plé, H., Duchez, A. C., Cloutier, N., Boilard, E., and Provost, P. (2013) Activated platelets can deliver mRNA regulatory Ago2*microRNA complexes to endothelial cells via microparticles. *Blood* **122,** 253–261
23. Duchez, A. C., Boudreau, L. H., Naika, G. S., Bollinger, J., Belleannée, C., Cloutier, N., Laffont, B., Mendoza-Villarroel, R. E., Lévesque, T., Rollet-Labelle, E., Rousseau, M., Allaeys, I., Tremblay, J. J., Poubelle, P. E., Lambeau, G., Pouliot, M., Provost, P., Soulet, D., Gelb, M. H., and Boilard, E. (2015) Platelet microparticles are internalized in neutrophils via the concerted activity of 12-lipoxygenase and secreted phospholipase A2-IIA. *Proc. Natl. Acad. Sci. U.S.A.* **112,** E3564–3573
24. Scott, R. S., McMahon, E. J., Pop, S. M., Reap, E. A., Caricchio, R., Cohen, P. L., Earp, H. S., and Matsushima, G. K. (2001) Phagocytosis and clearance of apoptotic cells is mediated by MER. *Nature* **411,** 207–211
25. Seitz, H. M., Camenisch, T. D., Lemke, G., Earp, H. S., and Matsushima, G. K. (2007) Macrophages and dendritic cells use different Axl/Mertk/Tyro3 receptors in clearance of apoptotic cells. *J. Immunol.* **178,** 5635–5642
26. Xiong, W., Chen, Y., Wang, H., Wang, H., Wu, H., Lu, Q., and Han, D. (2008) Gas6 and the Tyro 3 receptor tyrosine kinase subfamily regulate the phagocytic function of Sertoli cells. *Reproduction* **135,** 77–87
27. Lu, Q., Gore, M., Zhang, Q., Camenisch, T., Boast, S., Casagranda, F., Lai, C., Skinner, M. K., Klein, R., Matsushima, G. K., Earp, H. S., Goff, S. P., and Lemke, G. (1999) Tyro-3 family receptors are essential regulators of mammalian spermatogenesis. *Nature* **398,** 723–728
28. Vollrath, D., Feng, W., Duncan, J. L., Yasumura, D., D'Cruz, P. M., Chappelow, A., Matthes, M. T., Kay, M. A., and LaVail, M. M. (2001) Correction of the retinal dystrophy phenotype of the RCS rat by viral gene transfer of Mertk. *Proc. Natl. Acad. Sci. U.S.A.* **98,** 12584–12589
29. Grommes, C., Lee, C. Y., Wilkinson, B. L., Jiang, Q., Koenigsknecht-Tal-

boo, J. L., Varnum, B., and Landreth, G. E. (2008) Regulation of microglial phagocytosis and inflammatory gene expression by Gas6 acting on the Axl/Mer family of tyrosine kinases. *J. Neuroimmune Pharmacol.* **3,** 130–140
30. Rothlin, C. V., Ghosh, S., Zuniga, E. I., Oldstone, M. B., and Lemke, G. (2007) TAM receptors are pleiotropic inhibitors of the innate immune response. *Cell* **131,** 1124–1136
31. Sen, P., Wallet, M. A., Yi, Z., Huang, Y., Henderson, M., Mathews, C. E., Earp, H. S., Matsushima, G., Baldwin, A. S., Jr., and Tisch, R. M. (2007) Apoptotic cells induce Mer tyrosine kinase-dependent blockade of NF-κB activation in dendritic cells. *Blood* **109,** 653–660
32. Hafizi, S., and Dahlbäck, B. (2006) Gas6 and protein S. Vitamin K-dependent ligands for the Axl receptor tyrosine kinase subfamily. *FEBS J.* **273,** 5231–5244
33. Fraineau, S., Monvoisin, A., Clarhaut, J., Talbot, J., Simonneau, C., Kanthou, C., Kanse, S. M., Philippe, M., and Benzakour, O. (2012) The vitamin K-dependent anticoagulant factor, protein S, inhibits multiple VEGF-A-induced angiogenesis events in a Mer- and SHP2-dependent manner. *Blood* **120,** 5073–5083
34. Ruan, G. X., and Kazlauskas, A. (2012) Axl is essential for VEGF-A-dependent activation of PI3K/Akt. *EMBO J.* **31,** 1692–1703
35. Gallicchio, M., Mitola, S., Valdembri, D., Fantozzi, R., Varnum, B., Avanzi, G. C., and Bussolino, F. (2005) Inhibition of vascular endothelial growth factor receptor 2-mediated endothelial cell activation by Axl tyrosine kinase receptor. *Blood* **105,** 1970–1976
36. Hasanbasic, I., Cuerquis, J., Varnum, B., and Blostein, M. D. (2004) Intracellular signaling pathways involved in Gas6-Axl-mediated survival of endothelial cells. *Am. J. Physiol. Heart Circ. Physiol.* **287,** H1207–H1213
37. Healy, A. M., Schwartz, J. J., Zhu, X., Herrick, B. E., Varnum, B., and Farber, H. W. (2001) Gas 6 promotes Axl-mediated survival in pulmonary endothelial cells. *Am. J. Physiol. Lung Cell. Mol. Physiol.* **280,** L1273–L1281
38. Laurance, S., Aghourian, M. N., Jiva Lila, Z., Lemarié, C. A., and Blostein, M. D. (2014) Gas6-induced tissue factor expression in endothelial cells is mediated through caveolin-1-enriched microdomains. *J. Thromb. Haemost.* **12,** 395–408
39. Robins, R. S., Lemarié, C. A., Laurance, S., Aghourian, M. N., Wu, J., and Blostein, M. D. (2013) Vascular Gas6 contributes to thrombogenesis and promotes tissue factor up-regulation after vessel injury in mice. *Blood* **121,** 692–699
40. Angelillo-Scherrer, A., de Frutos, P., Aparicio, C., Melis, E., Savi, P., Lupu, F., Arnout, J., Dewerchin, M., Hoylaerts, M., Herbert, J., Collen, D., Dahlbäck, B., and Carmeliet, P. (2001) Deficiency or inhibition of Gas6 causes platelet dysfunction and protects mice against thrombosis. *Nat. Med.* **7,** 215–221
41. Ekman, C., Stenhoff, J., and Dahlbäck, B. (2010) Gas6 is complexed to the soluble tyrosine kinase receptor Axl in human blood. *J. Thromb. Haemost.* **8,** 838–844
42. Lundblad, R. L., Uhteg, L. C., Vogel, C. N., Kingdon, H. S., and Mann, K. G. (1975) Preparation and partial characterization of two forms of bovine thrombin. *Biochem. Biophys. Res. Commun.* **66,** 482–489
43. Stenhoff, J., Dahlbäck, B., and Hafizi, S. (2004) Vitamin K-dependent Gas6 activates ERK kinase and stimulates growth of cardiac fibroblasts. *Biochem. Biophys. Res. Commun.* **319,** 871–878
44. Dahlbäck, B. (1983) Purification of human vitamin K-dependent protein S and its limited proteolysis by thrombin. *Biochem. J.* **209,** 837–846
45. Dahlbäck, B., Hildebrand, B., and Malm, J. (1990) Characterization of functionally important domains in human vitamin K-dependent protein S using monoclonal antibodies. *J. Biol. Chem.* **265,** 8127–8135
46. Tsou, W. I., Nguyen, K. Q., Calarese, D. A., Garforth, S. J., Antes, A. L., Smirnov, S. V., Almo, S. C., Birge, R. B., and Kotenko, S. V. (2014) Receptor tyrosine kinases, TYRO3, AXL, and MER, demonstrate distinct patterns and complex regulation of ligand-induced activation. *J. Biol. Chem.* **289,** 25750–25763
47. MacDonald, R. C., MacDonald, R. I., Menco, B. P., Takeshita, K., Subbarao, N. K., and Hu, L. R. (1991) Small-volume extrusion apparatus for preparation of large, unilamellar vesicles. *Biochim. Biophys. Acta* **1061,** 297–303
48. Dahlbäck, B., Wiedmer, T., and Sims, P. J. (1992) Binding of anticoagulant vitamin K-dependent protein S to platelet-derived microparticles. *Biochemistry* **31,** 12769–12777
49. Dransfield, I., Zagórska, A., Lew, E. D., Michail, K., and Lemke, G. (2015) Mer receptor tyrosine kinase mediates both tethering and phagocytosis of apoptotic cells. *Cell Death Dis.* **6,** e1646
50. Gould, W. R., Baxi, S. M., Schroeder, R., Peng, Y. W., Leadley, R. J., Peterson, J. T., and Perrin, L. A. (2005) Gas6 receptors Axl, Sky and Mer enhance platelet activation and regulate thrombotic responses. *J. Thromb. Haemost.* **3,** 733–741
51. Cosemans, J. M., Van Kruchten, R., Olieslagers, S., Schurgers, L. J., Verheyen, F. K., Munnix, I. C., Waltenberger, J., Angelillo-Scherrer, A., Hoylaerts, M. F., Carmeliet, P., and Heemskerk, J. W. (2010) Potentiating role of Gas6 and Tyro3, Axl and Mer (TAM) receptors in human and murine platelet activation and thrombus stabilization. *J. Thromb. Haemost.* **8,** 1797–1808
52. Burkhart, J. M., Vaudel, M., Gambaryan, S., Radau, S., Walter, U., Martens, L., Geiger, J., Sickmann, A., and Zahedi, R. P. (2012) The first comprehensive and quantitative analysis of human platelet protein composition allows the comparative analysis of structural and functional pathways. *Blood* **120,** e73–82
53. Lew, E. D., Oh, J., Burrola, P. G., Lax, I., Zagorska, A., Traves, P. G., Schlessinger, J., and Lemke, G. (2014) Differential TAM receptor-ligand-phospholipid interactions delimit differential TAM bioactivities. *eLife* **3,** e03385
54. Manfioletti, G., Brancolini, C., Avanzi, G., and Schneider, C. (1993) The protein encoded by a growth arrest-specific gene (gas6) is a new member of the vitamin K-dependent proteins related to protein S, a negative coregulator in the blood coagulation cascade. *Mol. Cell. Biol.* **13,** 4976–4985
55. Fens, M. H., Mastrobattista, E., de Graaff, A. M., Flesch, F. M., Ultee, A., Rasmussen, J. T., Molema, G., Storm, G., and Schiffelers, R. M. (2008) Angiogenic endothelium shows lactadherin-dependent phagocytosis of aged erythrocytes and apoptotic cells. *Blood* **111,** 4542–4550
56. Koshiar, R. L., Somajo, S., Norström, E., and Dahlbäck, B. (2014) Erythrocyte-derived microparticles supporting activated protein C-mediated regulation of blood coagulation. *PLoS One* **9,** e104200
57. Wang, J. G., Williams, J. C., Davis, B. K., Jacobson, K., Doerschuk, C. M., Ting, J. P., and Mackman, N. (2011) Monocytic microparticles activate endothelial cells in an IL-1β-dependent manner. *Blood* **118,** 2366–2374
58. Nakano, T., Higashino, K., Kikuchi, N., Kishino, J., Nomura, K., Fujita, H., Ohara, O., and Arita, H. (1995) Vascular smooth muscle cell-derived, Gla-containing growth-potentiating factor for Ca^{2+}-mobilizing growth factors. *J. Biol. Chem.* **270,** 5702–5705
59. Zhu, D., Wang, Y., Singh, I., Bell, R. D., Deane, R., Zhong, Z., Sagare, A., Winkler, E. A., and Zlokovic, B. V. (2010) Protein S controls hypoxic/ischemic blood-brain barrier disruption through the TAM receptor Tyro3 and sphingosine 1-phosphate receptor. *Blood* **115,** 4963–4972
60. Chung, W. S., Clarke, L. E., Wang, G. X., Stafford, B. K., Sher, A., Chakraborty, C., Joung, J., Foo, L. C., Thompson, A., Chen, C., Smith, S. J., and Barres, B. A. (2013) Astrocytes mediate synapse elimination through MEGF10 and MERTK pathways. *Nature* **504,** 394–400
61. Subramanian, M., Hayes, C. D., Thome, J. J., Thorp, E., Matsushima, G. K., Herz, J., Farber, D. L., Liu, K., Lakshmana, M., and Tabas, I. (2014) An AXL/LRP-1/RANBP9 complex mediates DC efferocytosis and antigen cross-presentation *in vivo*. *J. Clin. Invest.* **124,** 1296–1308
62. Zagórska, A., Través, P. G., Lew, E. D., Dransfield, I., and Lemke, G. (2014) Diversification of TAM receptor tyrosine kinase function. *Nat. Immunol.* **15,** 920–928
63. Bertin, F. R., Lemarié, C. A., Robins, R. S., and Blostein, M. D. (2015) Growth arrest-specific 6 regulates thrombin-induced expression of vascular cell adhesion molecule-1 through forkhead box O1 in endothelial cells. *J. Thromb. Haemost.* **13,** 2260–2272
64. Miner, J. J., Daniels, B. P., Shrestha, B., Proenca-Modena, J. L., Lew, E. D., Lazear, H. M., Gorman, M. J., Lemke, G., Klein, R. S., and Diamond, M. S. (2015) The TAM receptor Mertk protects against neuroinvasive viral infection by maintaining blood-brain barrier integrity. *Nat. Med.* **21,** 1464–1472